Two consecutive microtubule-based epithelial seaming events mediate dorsal closure in the scuttle fly *Megaselia abdita*.

Juan J. Fraire-Zamora[1,2*], Johannes Jaeger[3,4] and Jérôme Solon[1,2*]

[1] Cell and Developmental Biology Programme, Centre for Genomic Regulation (CRG), The Barcelona Institute of Science and Technology, Dr. Aiguader 88, Barcelona 08003, Spain
[2] Universitat Pompeu Fabra (UPF), Barcelona 08003, Spain.
[3] EMBL-CRG Systems Biology Unit, Centre for Genomic Regulation (CRG), Dr. Aiguader 88, Barcelona 08003, Spain; Universitat Pompeu Fabra (UPF), Barcelona 08003, Spain.
[4] Current address: Complexity Science Hub Vienna, Josefstädter Straße 39, 1080 Vienna, Austria, yoginho@gmail.com

[*] Corresponding authors: Jerome.solon@crg.eu; juanjose.fraire@crg.eu

Abstract

Evolution of morphogenesis is generally associated with changes in genetic regulation. Here we report evidence indicating that dorsal closure, a conserved morphogenetic process in dipterans, evolved as the consequence of rearrangements in epithelial organization rather than signaling regulation. In *Drosophila melanogaster*, dorsal closure consists of a two-tissue system where the contraction of extraembryonic amnioserosa and a JNK/Dpp-dependent epidermal actomyosin cable result in microtubule-dependent seaming of the epidermis. We find that dorsal closure in *Megaselia abdita,* a three-tissue system comprising serosa, amnion and epidermis, differs in morphogenetic rearrangements despite conservation of JNK/Dpp signaling. In addition to an actomyosin cable, *M. abdita* dorsal closure is driven by the rupture and contraction of the serosa and the consecutive microtubule-dependent seaming of amnion and epidermis. Our study indicates that the evolutionary transition to a reduced system of dorsal closure involves simplification of the seaming process without changing the signaling pathways of closure progression.

Impact Statement

Evolutionary reduction in tissue number involves the simplification of the seaming process but not signaling during epithelial fusion.

Key words: *Megaselia abdita*, dorsal closure, microtubule cytoskeleton, extraembryonic tissue (serosa/amnion), tissue seaming, evolution of development (evo-devo)

47

48 **Introduction**

49 Mechanical forces produced at the cellular level are known to shape tissues during
50 morphogenesis (see Lecuit et al., 2011, for a recent review). Molecular motors and
51 cytoskeletal elements generate these mechanical forces, which cause tissues to deform
52 and change shape (Mammoto and Ingber, 2010). Until recently, such tissue-level
53 aspects of morphogenesis have received relatively little attention in the field of
54 evolutionary developmental biology. The evolution of developmental processes is
55 generally attributed to changes in genetic regulation (see for example, Carroll et al.,
56 2009; Davidson and Erwin, 2006; Peter and Davidson, 2015; Wilkins, 2002). To date,
57 it is not fully understood how a developing organism integrates the mechanical and
58 genetic factors necessary to shape a tissue, or how this interplay between tissue
59 mechanics and genetics is contributing to the evolution of development. We focus on
60 this latter aspect by studying how a continuous epidermal layer is formed by epithelial
61 fusion during dorsal closure in a non-model organism, the scuttle fly *Megaselia*
62 *abdita* (Diptera: Phoridae).

63

64 Epithelial fusion is a fundamental morphogenetic mechanism in animal development
65 where two opposing epithelial sheets are brought together to subsequently seam and
66 result in a single continuous epithelial layer (Jacinto et al., 2001). Dorsal closure in
67 *Drosophila melanogaster* (Diptera: Drosophilidae) is a classical model system to
68 study epithelial fusion (Jacinto et al., 2000). This process is promoted by the
69 mechanical action of different players: a contractile actomyosin cable forming at the
70 leading edge of the epidermal flanks, the extraembryonic amnioserosa which covers
71 the dorsal opening and generates contractile forces during epidermal flank

advancement, and the eventual seaming of the epidermis through a mechanism involving microtubule-based cellular protrusions (Eltsov et al., 2015; Hutson et al., 2003; Kiehart et al., 2000; Saias et al., 2015). Genetically, the c-Jun N-terminal kinase (JNK) pathway and the transforming growth factor beta (TGF-β) family gene *decapentaplegic* (*dpp*) play an essential regulatory role in the process (Fernandez et al., 2007; Glise and Noselli, 1997; Jacinto et al., 2002; Knust, 1997). The expression of *dpp* localizes to the leading edge of the epidermal flanks and depends on the activity of the *D. melanogaster* JNK gene (*basket*, *bsk*). Embryos lacking *bsk* activity show downregulation of *dpp* at the epidermal leading edge, failure of dorsal closure progression, and a dorsal-open phenotype in the larval cuticle (Glise and Noselli, 1997; Sluss et al., 1996). At the molecular level, activation of the JNK/Dpp signaling pathways promotes the formation and maintenance of the actomyosin cable at the epidermal leading edge (Ducuing et al., 2015) and, thus, progression of the opposing epidermal flanks towards the dorsal midline where they meet. At the final stage of dorsal closure, the opposing epidermal flanks "zipper" or "seam" through the action of microtubules that align towards the dorsal opening and promote the formation of filopodial protrusions at both epidermal leading edges (Jacinto et al., 2002; Jankovics and Brunner, 2006; Millard and Martin, 2008).

Dorsal closure is a conserved morphogenetic process that occurs in all insects (Chapman, 1998). Whereas in *D. melanogaster* it involves two tissues, the embryonic epidermis and the extraembryonic amnioserosa, in most insects it involves three: the embryonic epidermis, an extraembryonic amnion, and a separate extraembryonic serosa (Panfilio, 2008; Schmidt-Ott and Kwan, 2016). These complex anatomical differences raise the question whether the mechanisms responsible for epithelial

97 fusion in a simple two-tissue system are conserved in a three-tissue system. The
98 phorid scuttle fly *M. abdita* (placed in an early-branching cyclorraphan lineage)
99 presents a three-tissue system of dorsal closure and has been established as a model to
100 study the evolution of developmental processes (Bullock et al., 2004; Rafiqi et al.,
101 2008; Schmidt-Ott et al., 1994; Stauber et al., 2000; Wotton et al., 2015). Thus, *M.*
102 *adbita* offers the opportunity to compare the three-tissue system of dorsal closure to
103 the two-tissue system present in *D. melanogaster*.
104
105 Here, we perform a quantitative characterization of dorsal closure in *M. abdita*.
106 Combining molecular tools with live imaging, we show that dorsal closure in
107 *M. abdita* embryos occurs in three distinct phases: (i) serosa rupture and retraction,
108 (ii) serosa contraction and progression of opposing epidermal flanks, and (iii) a dual
109 seaming process to eventually form a fused continuous epidermis. Despite the
110 significant morphological differences with *D. melanogaster*, the regulation of dorsal
111 closure in *M. abdita* involves a conserved role for the JNK/Dpp signaling pathway to
112 form and maintain an epidermal actomyosin cable surrounding the dorsal opening.
113 More specifically, we find that following an actomyosin-dependent contraction of the
114 serosa, two consecutive microtubule-dependent seaming events take place in the
115 amnion as well as in the epidermis. In both cases, apical microtubule bundles align
116 and extend towards the site of closure suggesting a general epithelial fusion
117 mechanism. Altogether, our results provide a dynamic and quantitative description of
118 epithelial fusion in a complex three-tissue system. They indicate that the evolutionary
119 transition from a three-tissue to a two-tissue system of dorsal closure involves
120 changes in the number and sequence of morphogenetic events, rather than changes in

121 the spatio-temporal activity of the main signaling pathways that control closure
122 progression.
123
124 **Results**
125 **Dorsal closure in *Megaselia abdita* involves synchronized serosa rupture and**
126 **epidermal progression.**
127 In order to map the spatial arrangement of tissues involved in dorsal closure of
128 *M. abdita* embryos, we obtained confocal projections of fixed non-devitellinized
129 embryos with stained nuclei. Nuclear anatomy and staining have been used previously
130 to identify extraembryonic tissues in the flour beetle *Tribolium castaneum* (Panfilio *et*
131 *al*, 2013). In *M. abdita*, staining fixed embryos with the nuclear dye DAPI allowed us
132 to distinguish three types of tissues: (*1*) The extraembryonic serosa, which constitutes
133 the outermost extraembryonic layer and envelops the entire *M. abdita* embryo before
134 the onset of dorsal closure (magenta in figure 1A, 1A' and 1B, B'). Its cells have very
135 large nuclei (average size 125± 21 μm^2, SD, *n*=150 cells) and show discontinuous or
136 "punctuated" DAPI staining (magenta in figure 1A, 1A' and figure 1— supplement
137 1A-A' and B-B''). (*2*) The extraembryonic amnion, which is 1–2 cells wide, localizes
138 in between the serosal and epidermal tissues (blue in figure 1A, 1A' and 1B, B'). Its
139 cells also have large nuclei (average size 77 ± 16 μm^2, SD, *n*=150 cells) and show a
140 more continuous, "compact" DAPI staining (blue in figure 1A, 1A' and figure 1—
141 supplement 1A-A' and B-B''). (*3*) The embryonic epidermis, which contains
142 numerous small nuclei (average size 14 ± 3 μm^2, SD, *n*=150 cells) that are tightly
143 packed (gray in figure 1A and A').
144

In order to obtain a closer view of the spatial arrangement of tissues in live *M. abdita* embryos, we injected DAPI at the embryo poles during dorsal closure stage and obtained confocal projections. This staining showed that amnion cells sit on top of yolk granules, and are positioned adjacent to the embryonic epidermis (blue arrowheads in figure 1— supplement 1C-C").

When fixing *M. abdita* embryos at dorsal closure stage, devitellinization also removes the serosa together with the vitelline membrane (figure 1— supplement 2A). Devitellinization and serosa cells removal resulted in a gap on the dorsal side of the embryo, seen as lack of phalloidin staining (figure 1— supplement 2B). Amnion cells (1–2 cell rows adjacent to the epidermis, blue arrowheads in figure 1— supplement 2B) remained apposed to an intact epidermis. In a few cases, devitellinization left some intact serosa cells on top of *M. abdita* embryos (very large cells highlighted by phalloidin and DAPI counterstains, white arrowhead in figure 1— supplement 2C and C'). An optical re-slice of confocal projections of the intact serosa and amnion cells showed that these two cells types are apposed (yellow arrowhead in figure 1— supplement 2C'').

In summary, the anatomy of *M. abdita* embryos at dorsal closure reveals a three-tissue system, where large serosa cells surround the embryo and are apposed to the amnion cells at the dorsal-most end of the embryo. Amnion cells form a row, in turn apposed to the adjacent epidermis (figure 1B and B'). This three-tissue geometry poses an interesting challenge for the process of dorsal closure, since the apposed serosa and amnion need to undergo dramatic rearrangements to achieve epidermal fusion at the end of dorsal closure.

How does *M. abdita* solve this problem? At early stages of dorsal closure, the serosa surrounding the embryo undergoes an abrupt rupture (Wotton et al., 2014). Serosa rupture initiates close to the posterior pole of the embryo. Spread of the rupture occurs anteriorly through the ventral side of the embryo and results in a retraction of the serosa towards the dorsal end of the embryo (figure 1C). During this process, serosa cells accumulate at the dorsal opening (magenta arrowheads in figure 1D, and magenta cells in 1G-G''). In the meantime, the amnion remains in place, apposed to the serosa (blue arrowheads in figure 1D, and blue cells in 1G-G''), and adjacent to the embryonic epidermis (white arrowheads in figure 1D, and green line in 1G-G'').

To gain quantitative evidence on the dynamics of dorsal closure in *M. abdita*, we labeled live embryos with the fluorescent lipophylic dye FM 4-64 and followed the process using confocal imaging (video 1). We used the fusion of the dorsal ridge (merging of the ridge primordia at the dorsal midline, magenta bar in figure 1— supplement 3A and A') as a developmental landmark for the initiation of dorsal closure (*T=0* min) (Campos-Ortega and Hartenstein, 1997; VanHook and Letsou, 2008). Under this time frame, the serosa ruptures at *T=25* min (±*8* min, SD; *n=15* embryos) and dorsal closure (seaming of the embryonic epidermal flanks at the dorsal midline, see yellow line in figure 1— supplement 3A'') concludes at *T=74* min (±*10* min, SD, *n=15* embryos).

To relate serosa retraction to the kinetics of dorsal closure, we measured the relative changes in area of the serosa covering the embryo and the relative changes in height (*h*) of the dorsal opening over time (see red and blue curves in figure 1F, yellow

195 dashed line in figure 1E, blue line in figure 1— supplement 3A- and Materials and
196 Methods). At *early* stages of dorsal closure, the leading edge of the epidermis
197 straightens (yellow line in figure 1— supplement 3A, 3A'') and the dorsal opening
198 increases progressively in height (*h*) (blue curve in figure 1F). After dorsal ridge
199 fusion (pink area in figure 1F), the serosa ruptures, retracts and accumulates onto the
200 dorsal opening (figure1C, magenta arrowheads in 1D, yellow dashed line in 1E,
201 magenta cells in 1G'-G''). This is concurrent with a fast reduction in dorsal opening
202 height (red and blue curves in figure 1F, yellow line in figure 1— supplement 3A'-
203 A''). Visualizing the process from an orthogonal view, we observe that following
204 serosa accumulation on top of the dorsal opening, this extraembryonic tissue bends
205 inwards and serosa cells undergo an apicobasal elongation resulting in the
206 internalization of a large part of the serosa cells into the yolk prior to epidermal fusion
207 (video 2 and figure 1— supplement 3B and 3C-C'). At *late* dorsal closure stages, the
208 serosa is fully internalized (magenta cells in figure 1G'') and the two epidermal flanks
209 continue progressing towards the dorsal midline, covering the dorsal opening and
210 eventually fusing completely (figure 1— supplement 3A'').
211
212 **Inhibition of JNK/Dpp signaling in *Megaselia abdita* arrests dorsal closure but**
213 **not serosa rupture.**
214 Since the JNK and Dpp signaling pathways are known to regulate dorsal closure in
215 *D. melanogaster* embryos, and their impairment results in the failure of dorsal closure
216 and in a dorsal-open phenotype (Glise and Noselli, 1997; Sluss et al., 1996), we
217 wondered whether JNK and Dpp signaling would also be important regulators of
218 dorsal closure and serosa retraction in *M. abdita* embryos. Using *in situ* hybridization
219 and cuticle preparations, we observed that in wild-type embryos, *M. abdita dpp*

(*Mab_dpp*) is expressed along the leading edge of the epidermis (black arrowheads in figure 2A) and progression of dorsal closure results in the deposition of a continuous larval cuticle (figure 2A'), very similar to *D. melanogaster*. Next, we perturbed the *M. abdita* JNK pathway, using gene knockdown by RNA interference (RNAi, see Materials and Methods) against *M. abdita bsk* (*Mab_bsk*) in pre-gastrulating embryos. Around 90% of *Mab_bsk* dsRNA-injected embryos developed to at least germband retraction stage (821 out of 922 embryos). *Mab_bsk* RNAi knock-down resulted in both a disrupted pattern of *Mab_dpp* expression (including a complete absence of expression at the leading edge of the epidermis, magenta arrowheads in figure 2B) and a dorsal-open phenotype in the larval cuticle (magenta arrowheads in figure 2B') of ~64% of RNAi-injected and developed embryos (528 out of 821 embryos). Both phenotypes are similar to the ones that occur in *D. melanogaster* embryos after JNK/Dpp signaling perturbation. Interestingly, live imaging of RNAi-injected embryos reveals that serosa rupture and retraction still occur (yellow dashed line in figure 2C–C'' and video 3), despite a failure of progression of the epidermal flanks (yellow arrowheads in figure 2— supplement 1B; note that the embryo from video 3 and figure 2C corresponds to the same embryo in figure 2— supplement 1B, 24 hours after RNAi injection). In summary, these results indicate that JNK and Dpp signaling regulate progression of dorsal closure in *M. abdita* as in *D. melanogaster* embryos, but are not required for the regulation of serosa rupture and retraction.

Actomyosin contractility in the serosa and an actomyosin epidermal cable are necessary for dorsal closure in *Megaselia abdita* embryos.

In *D. melanogaster* embryos, both a JNK/Dpp-dependent contractile epidermal cable and the contraction of the amnioserosa tissue (through actomyosin contractility and

245 volume decrease) power the progression of dorsal closure (Hutson et al., 2003;
246 Kiehart et al., 2000; Saias et al., 2015). The actomyosin cytoskeleton is therefore an
247 essential component in force generation during this process. To gain insights into the
248 structures generating forces during dorsal closure in *M. abdita*, we stained fixed
249 embryos with phalloidin (to reveal F-actin) or a phosphoMyosin antibody. Both stains
250 showed accumulation at the leading edge of the epidermis (green arrowheads in figure
251 3A and 3B) and at the surface of serosa cells during internalization (red arrowheads in
252 figure 3A and 3B). Measurements from time-lapse sequences showed that serosa cell
253 area reduces over time during their accumulation at the dorsal opening, from an
254 average of 212 ± 52 μm^2 (SD; *n*=20 cells) to 76 ± 18 μm^2 (SD; *n*=20 cells) to 33 ±
255 μm^2 (SD; *n*=20cells) at 20, 30 and 40 min after serosa rupture, respectively (figure
256 3— supplement 1B). This cell area reduction correlates with an apical accumulation
257 of actin at early stages of serosa internalization (white arrowheads in figure 3—
258 supplement 1c-c''), suggesting an apical constriction mechanism through actomyosin
259 contraction during serosa internalization. In contrast, amnion cells show low levels of
260 actin and myosin, even during late stages of dorsal closure after full serosa
261 internalization (blue arrowhead in figure 3A and 3B, figures 3 C'' and figure 3—
262 supplement 1A). Closer observation also reveals the presence of actin-enriched
263 filopodia-like extensions protruding from the actomyosin cable (yellow arrowheads in
264 figure 3— supplement 1D and D'). RNAi knock-down of *Mab_bsk* strongly reduces
265 the level of actin accumulation at the epidermal leading edge compared to wild-type
266 embryos (white arrows in figure 3— supplement 2A and B). This suggests that the
267 embryonic epidermal cable is similar in structure and regulated by the JNK/Dpp
268 signaling pathway in both *M. abdita* and *D. melanogaster* embryos.
269

A timed sequence of phalloidin-stained *M. abdita* embryos (figure 3C–C’’’) reveals further details concerning the dynamics of dorsal closure: upon serosa internalization, the amniotic flanks (devoid of actomyosin) move to the dorsal midline where the two flanks merge (white arrowhead in figure 3C’’). Upon merging of amnion flanks, the actomyosin cable propels the epidermal flanks to the dorsal midline where epidermal seaming takes place (yellow arrowheads in figure 3C’, C’’ and C’’’).

To affect actomyosin-based tissue contractility, we injected *M. abdita* embryos with the Rho kinase (ROCK) inhibitor Y-27632. This drug has been extensively used in *D. melanogaster* to inhibit actomyosin contractility by blocking ROCK activity and, consequently, downstream targets including myosin phosphorylation (Czerniak et al., 2016; Monier et al., 2010; Sommi et al., 2011). Injection of Y-27632 at early stages of *M. abdita* dorsal closure reduces actomyosin accumulation at the epidermal leading edge compared to wild-type embryos (white arrowheads in figure 3— supplement 2A and C). The progression of the epidermal leading edge is arrested upon treatment (figure 3— supplement 2D-D’’ and video 4). The internalization of serosa cells is also abolished as observed by the lack of inward bending and apicobasal elongation of this tissue in orthogonal view (figure 3— supplement 2E-E’’ and video 5). These observations indicate that actomyosin contractility contributes to both the internalization of the serosa and progression of the epidermal leading edge. Interestingly, the kinetics of serosa retraction in Y-27632-injected embryos seemed less affected during the first half of the process than the second half (purple curve in figure 3D), suggesting that actomyosin-based cell contraction is taking place mainly at the final stage of retraction and during serosa internalization.

Taken together, these results indicate that actomyosin-based contractility within the serosa and the cable surrounding the dorsal opening are required for the progression of dorsal closure in *M. abdita* embryos.

A microtubule-based seaming of the extraembryonic amnion is required for dorsal closure in *Megaselia abdita* embryos.

In addition to an actomyosin cable, the microtubule cytoskeleton is known to be essential during the last step of dorsal closure in *D. melanogaster*. In epidermal cells at the leading edge, microtubules align in apical bundles parallel to the dorsoventral axis and protrude into stable filopodia. These aligned epidermal microtubules are required for proper epidermal seaming and their depolymerization leads to defects in seaming and incomplete closure in *D. melanogaster* (Jankovics and Brunner, 2006). We investigated whether such a microtubule configuration is observable during dorsal closure in *M. abdita* as well. Staining fixed *M. abdita* embryos at different stages of *late* dorsal closure with a β-tubulin antibody, we observed that microtubules in the epidermis also orient towards the dorsal midline (figure 4— supplement 1A and B) and protrude from the epidermal leading edge (white arrowheads in figure 4— supplement 1B) forming apical bundles (figure 4— supplement 1B'). This epidermal microtubule alignment is maintained throughout epidermal flank advancement and during epidermal seaming (figure 4— supplement 1C-C'''). Interestingly, we find a similar alignment of microtubules in the extraembryonic amnion, where microtubule bundles localize apically (figure 4B') and orient towards the internalizing serosa (blue arrowheads in figure 4A and B and figure 4— supplement 1A). This apical microtubule alignment in the amnion seems to follow cell elongation. To support this observation, we estimated apical cell surface area by performing a Voronoi

320 tessellation around the nuclei of extraembryonic cells. We could observe that amniotic
321 cells present an elongated apical cell surface area (285 ± 81µm^2, SD; *n*=12 cells; blue
322 arrowheads in figure 4— supplement 1D) compared to serosa cells (57 ± 23 µm^2, SD;
323 *n*=108 cells; red arrowheads in figure 4— supplement 1D). Both apical microtubule
324 alignment and elongated apical cell surface area in the amnion are maintained during
325 serosa internalization and merging of amnion cells from opposite flanks (blue
326 arrowheads in figure 4B and figure 4— supplement 1C-C'). Amnion microtubule
327 alignment is subsequently lost after the opposite amnion flanks meet at the dorsal
328 midline (blue arrowhead in figure 4— supplement 1C'').
329
330 Since microtubule alignment is necessary for epidermal seaming during dorsal closure
331 in *D. melanogaster*, we reasoned that a similar microtubule alignment in the amnion
332 of *M. abdita* embryos could indicate epithelial amniotic fusion through seaming in
333 this species. To follow the last steps of *M. abdita* dorsal closure more closely, we
334 imaged FM 4-64-labeled embryos during the *late* stage of dorsal closure (video 6).
335 We observed that upon serosa internalization, the opposing amniotic flanks of
336 *M. abdita* embryos meet and fuse at the dorsal midline, suggesting an amniotic
337 seaming process (blue-shaded area in figure 4C, C' and C''). Immediately after
338 amniotic seaming occurred, the epidermal flanks progressed dorsally and also seamed
339 on top of the continuous amnion (green dashed line in figure 4C, C' and C''). An
340 estimation of seaming velocities in the amnion and epidermis (8.1 ± 2 µm/min and 3.8
341 ± 1.7 µm/min, SD, *n*= 5 embryos, respectively) shows a variation in speed between
342 the two processes that could result from a difference in the mechanical properties of
343 the fusing epithelia or the seaming angle at each canthi.
344

345 To investigate the functional role of microtubules in amnion cell elongation and
346 seaming, we injected embryos with the microtubule depolymerizing drug colcemid
347 (Jankovics and Brunner, 2006). Injection of colcemid does not perturb the kinetics of
348 serosa retraction (figure 4— supplement 2A), actin accumulation in serosa cells (red
349 arrowheads in figure 4— supplement 2B and B'), straightening of the epidermal
350 leading edge (white arrowheads in figure 4D), or actin cable formation (white
351 arrowheads in figure 4— supplement 2B and B'). An orthogonal view from a time-
352 lapse sequence also shows that the initial inward bending and apicobasal elongation of
353 the serosa cells during internalization occurs in both wild type and colcemid injected
354 embryos (video 7 and magenta dashed lines in figure 1— supplement 3C-C' and
355 figure 4— supplement 2C-C').
356
357 In contrast, dorsal closure arrests during the internalization of the serosa (red
358 arrowhead in figure 4D'') and does not progress towards epithelial seaming (video 8
359 and red curve in figure 4E). We observe that microtubule polymerization does not
360 occur in colcemid-injected embryos (blue and white arrowheads for amnion and
361 epidermal cells, respectively, in figure 4— supplement 2D compared to 2D') and that
362 amnion cells initially elongate towards the dorsal midline as in wild type conditions,
363 although they relax and retract from the amnion merging site (figure 4— supplement
364 4A and video 9). In order to test the role of the microtubule assembly, specifically in
365 the amnion, we deactivated the depolymerizing effect of colcemid treatment on dorsal
366 closure progression with UV light. UV-irradiation was performed in a region between
367 the epidermis and the internalizing serosa, corresponding to the amnion (magenta area
368 in figure 4— supplement 3A''). In UV-irradiated embryos, dorsal closure progressed
369 further, reducing the height (*h*) of the dorsal opening, compared to colcemid treated

370 embryos, although it did not progress to the extent of wild type control embryos
371 (figure 4— supplement 3B). Taken together, these observations indicate that the
372 microtubule cytoskeleton in the amniotic tissue is required for seaming of the amnion
373 and the completion of dorsal closure.
374
375 In summary, the results presented in this section indicate the presence of subsequent
376 microtubule-based seaming processes in both the amnion and the epidermis during
377 dorsal closure in *M. abdita*. First, opposing amniotic flanks fuse at the dorsal midline
378 upon serosa ingression, followed by epidermal seaming (see schematics in figure 4F
379 and F' and lower panels of figure 4— supplement 4b–b''). Both of these processes are
380 necessary for the completion of epidermal seaming and dorsal closure, to result in a
381 continuous embryonic epidermal sheet.
382
383
384 **Discussion**
385 In this study, we provide a detailed characterization of epithelial fusion during dorsal
386 closure in the non-drosophilid scuttle fly *M. abdita*. In this species, dorsal closure
387 involves three different tissues: the embryonic epidermis, as well as the
388 extraembryonic amnion and serosa. Dorsal closure in *M. abdita* occurs in three
389 distinct phases: (i) rupture and retraction of the extraembryonic serosa surrounding
390 the embryo, (ii) concurrent contraction of both an epidermal actomyosin cable and the
391 serosal tissue in the dorsal region of the embryo leading to internalization of the
392 serosa into the dorsal opening, and (iii) successive seaming processes fusing first the
393 amnion and then the epidermis. Even though genetic regulation of dorsal closure by
394 the JNK and Dpp signaling pathways appears to be conserved between *M. abdita* and

395 *D. melanogaster*, the sequence of morphogenetic rearrangements is very different
396 between the two species. These differences, however, result in the same output: a
397 continuous epidermal layer covering the dorsal region of the embryo.
398
399 In *M. abdita*, the serosa encloses the whole embryo. It is apposed to the amnion,
400 which in turn is apposed to the epidermis at the edge of the dorsal opening
401 (schematics in figure 1B and B') (see also Rafiqi et al., 2008). The rupture of the
402 serosa is the first step of a series of complex morphogenetic events. Although the
403 initiation signal for serosal rupture is not yet known, we can discard a purely
404 mechanical trigger since injection of the embryo prior to dorsal closure did not induce
405 serosal rupture and global retraction, despite resulting in a small wound and a slight
406 retraction of the tissue around the injection site. In addition, rupture still occurs in
407 embryos injected with Rho-kinase (ROCK) inhibitor, which reduces actomyosin
408 contractility. Lastly, rupture always initiates at a very specific ventral-posterior site.
409 Taken together, these observations indicate that rupture is not triggered exclusively by
410 global straining and non-autonomous forces applied to the serosa tissue. Instead,
411 rupture seems to be triggered by a specific localized cue.
412
413 Upon rupture, the remaining serosal tissue retracts and constricts dorsally through an
414 actomyosin-dependent mechanism, in a way similar to serosa rupture and retraction in
415 the beetle *T. castaneum* (Hilbrant et al., 2016; Panfilio et al., 2013). The retracting
416 serosa then internalizes into the dorsal opening of *M. abdita*. Concomitant with
417 serosal internalization, a JNK/Dpp-dependent actomyosin cable forms at the
418 epidermal leading edge of *M. abdita* embryos. It promotes the advancement of the
419 opposing epidermal flanks towards the dorsal midline, and the eventual seaming of

420 the two flanks. This stage of dorsal closure occurs in a similar fashion to
421 *D. melanogaster*, but differs in comparison with *T. castaneum*, where no actomyosin
422 epidermal cable appears to be involved in epidermal flank advancement (Panfilio et
423 al., 2013).
424
425 In contrast to *D. melanogaster*, dorsal closure in *M. abdita* involves an additional
426 amniotic seaming process. Our experimental data indicate that amniotic seaming is
427 microtubule-dependent and essential for dorsal closure to occur. Thus, similar to
428 epidermal seaming in *D. melanogaster* embryos, where microtubules align
429 dorsoventrally prior to tissue fusion (Jankovics and Brunner, 2006), the two
430 sequential amniotic and epidermal seaming processes in *M. abdita* also involve a
431 dorsoventral alignment of microtubules.
432
433 Why microtubules align in this way remains unclear. One possible scenario is that
434 shape elongation of amniotic cells towards the retracting and internalizing serosa
435 could promote microtubule reorientation in the direction of contractile cells.
436 Interestingly, cellular fusion in the developing trachea of *D. melanogaster* involves
437 cell elongation and microtubules orientation towards the site of fusion (Kato et al.,
438 2016). Elongation of cells towards a contractile tissue also occurs during gastrulation
439 in *D. melanogaster* (Rauzi et al., 2015) and neural tube closure in the chordate *Ciona*
440 *intestinalis* (Hashimoto et al., 2015). It is not known whether microtubule alignment
441 also occurs in the latter processes to promote epithelial fusion. If this is the case, the
442 microtubule-dependent seaming that we describe might reflect a common mechanism
443 for epithelial tissues to fuse.
444

445 It remains unclear whether microtubule-dependent epithelial seaming is a process that
446 can generate forces contributing to dorsal closure. In the case of *D. melanogaster*,
447 laser-ablation of epidermal canthi (*i.e.* the epidermal corners where opposing
448 epidermal flanks meet) slows down the last stages of dorsal closure (Wells et al.,
449 2014). However, F-actin-enriched epidermal seaming still occurs between the
450 opposing leading edges of the epidermis despite the removal of the canthi.
451
452 Dorsal closure in embryos of *M. abdita* presents two sequential seaming events that
453 share a common feature: transient microtubule reorganization. It would be interesting
454 to explore if the cytoskeletal basis (*i.e.* microtubule reorganization) of epithelial
455 seaming events is conserved in other insect species with a three-tissue system of
456 dorsal closure, for example *T. castaneum*.
457
458 Our work suggests that the evolutionary transition from a three-tissue to a two-tissue
459 system of dorsal closure not only involves the reduction of extraembryonic tissue, *e.g.*
460 from distinct amnion and serosa to a fused amnioserosa (see Horn et al., 2015; Rafiqi
461 et al., 2008; Rafiqi et al., 2010; Schmidt-Ott and Kwan, 2016). In addition, it requires
462 changes in epidermal progression and seaming events. Further development of
463 imaging and molecular tools in *M. abdita* will help us better understand the
464 subcellular, cellular, and tissue dynamics that led to this evolutionary transition.
465
466 In the case of dipteran dorsal closure, it appears that the evolutionary modulation of
467 tissue remodeling is mainly driven by morphological rearrangements rather than large
468 changes in gene expression. This study provides the first detailed analysis of tissue
469 anatomy and dynamics complemented with gene expression assays to understand the

evolution of a morphogenetic process. In this respect, dipterans provide a powerful model to understand the interplay between tissue rearrangement and gene expression during the evolution of development.

Material and Methods

Fly Husbandry, Embryo Collection, Cloning Procedures, and RNAi knock-down.

Our *M. abdita* fly culture was maintained as previously described (Rafiqi et al., 2011a). Embryos were collected at 25°C for 4 hrs, and then incubated at 19°C until they reached stages 13–15, corresponding to dorsal closure as described in Wotton et al. (2014). *Mab_bsk* was cloned using sequence data from a published early embryonic transcriptome (http://diptex.crg.es; gene ID: *Mab_bsk*: MK10) (Jimenez-Guri et al., 2013). Briefly, open reading frames (ORFs) were PCR-amplified based on cDNA from 0–5hr-old *M. abdita* embryos. Amplified fragments were cloned into PCRII-TOPO (Invitrogen) or pGEM-T (Promega) vectors using the following specific primers (5'/3'): *Mab_bsk*, TGCCCGTCATCAGTTTTACA and GACGACGCGGGACTACTTTA. dsRNA was performed using the Ambion MEGAscript kit (Life Technologies). The following specific primers (5'/3') containing a T7 promoter sequence at their 5' end were used: *Mab_bsk*, GGTGGGCGACACAAGATT and AAACAGGCATCGGGGAAT. RNAi injection was performed using previously published protocols (Rafiqi et al., 2008; Rafiqi et al., 2010, 2011d; Wotton et al., 2015). Dechorionated embryos were injected prior to gastrulation at a concentration of 5 µM for *Mab_bsk*, then incubated at 25°C. The

injected dsRNA construct comprised 798 nucleotides (base pairs 369–1166 of the ORF) for *Mab_bsk*.

In Situ Hybridization, Immunohistochemistry, and Cuticle Preparations.

In situ hybridization in heat-fixed *M. abdita* embryos was performed according to a previously published protocol from *D. melanogaster* (Crombach et al., 2012). Digoxigenin-labeled *Mab_dpp* probe is from Jiménez-Guri et al. (2013). Fixation, devitellinization and immunostaining of *M. abdita* embryos were performed as previously described (Rafiqi et al., 2011c; Rafiqi et al., 2012) with slight modifications. Briefly, embryos undergoing dorsal closure were dechorionated and fixed for 25 min in heptane and PEMS (100 mM PIPES, 2 mM EGTA and 1 mM $MgSO_4$, pH 6.9), in a 3:1 PEMS:methanol solution, and a final concentration of 6.5% formaldehyde. Embryos were postfixed and hand devitellinized as described (Rafiqi et al., 2012). Microtubules were stained using a monoclonal primary antibody (mouse) against β-tubulin (E7, Developmental Studies Hybridoma Bank) at a dilution 1:100, and a secondary antibody conjugated to Alexa 488 dye (Invitrogen) at a dilution of 1:1000. For phalloidin staining, embryos were fixed for 1 hr using PEMS and a final concentration of 8% formaldehyde, hand-devitellinized as described for *D. melanogaster* embryos (Fernandez et al., 2007; Kaltschmidt et al., 2002; Rothwell and Sullivan, 2000), and incubated with phallodin-Alexa488 or phalloidin-Alexa563 (Invitrogen) at a dilution of 1:200 for 1 hr. When double-staining against phalloidin and microtubules, embryos were fixed, hand-devitellinized, and stained for phalloidin first, followed by incubation with the β-tubulin primary and secondary antibodies as above. Nuclei were counterstained using DAPI (1:1000). Embryos were washed in PBT (PBS, with 0.1% Triton X-100), and mounted using ProLong Gold Antifade

519 (Invitrogen). Cuticle preparations of *M. abdita* embryos were performed as previously
520 described (Rafiqi et al., 2011b) with slight modifications. Briefly, embryos were fixed
521 and hand-devitellinized before preparing and mounting the cuticles. Images of cuticle
522 preparations were taken using a phase-contrast microscope.
523
524 **Microscopy, Live Imaging, Pharmacology, UV irradiation, and Image**
525 **Processing.**
526 Time-lapse imaging was performed with dechorionated *M. abdita* embryos. RNAi-
527 injected embryos were imaged using a Zeiss Cell Observer with a controlled
528 temperature chamber at 25°C and phase contrast settings. For fluorescence imaging,
529 wild type embryos at dorsal closure stage were desiccated for 5 min, aligned, oriented,
530 and immobilized on a coverslip with heptane glue, covered with halocarbon oil and
531 injected at the embryo poles with 1 mM (needle concentration) of the lipophilic dye
532 FM 4-64 (Molecular Probes). Embryos were imaged at room temperature using an
533 Andor Revolution XD spinning-disk confocal microscope. ROCK inhibitor Y-27632
534 (Sigma) and colcemid (Santa Cruz Biotech) were prepared to 10 mM and 500 µg/ml
535 (needle concentration), and also injected at the embryo poles during dorsal closure
536 stage. Control embryos were injected with water or DMSO, respectively. Final needle
537 concentrations of dye and/or drugs were prepared in injection buffer (10 mM HEPES,
538 180 mM NaCl, 5 mM KCl and 1 mM $MgCl_2$, pH 7.2), and delivered to the interstitial
539 space formed between the serosa and the embryo. Confocal projections of ~10 *z*-stack
540 images (1 µm spacing) were used to generate time-lapse sequences in dorsal view.
541 Orthogonal views from time-lapse live imaging were obtained by reslicing confocal *z*-
542 stacks of 0.25 µm spacing. The height (*h*) of the dorsal opening is the maximum
543 perpendicular distance from the dorsal midline to the epidermal leading edge (Hutson

544 et al., 2003). The changes in area of the serosa covering the embryo over time were
545 determined by approximating the embryonic shape using an ellipse and resizing
546 manually to follow the serosa edge on one lateral side during retraction, assuming that
547 serosa retraction occurs symmetrically on both sides of the embryo after rupture along
548 the ventral midline. Detection of serosal edge morphology from bright-field time-
549 lapse sequences was performed by subtracting images at time t+1 from images at time
550 t. This operation rendered the contour of the retracting serosa visible. The
551 identification of extraembryonic tissues was performed using nuclear anatomy,
552 staining profiles and z position of the nuclei in confocal stack images obtained from
553 fixed embryos labeled with DAPI. Staining profiles, nuclear areas and z position in
554 the embryo were measured in 150 cells for each cell type (serosa and amnion) from
555 15 different embryos. UV irradiation experiments to deactivate colcemid were
556 performed as follows: dechorionated, desiccated, FM 4-64 labeled and colcemid -
557 injected *M. abdita* embryos were immobilized in heptane glue, mounted in halocarbon
558 oil, and imaged dorsally in an inverted Leica TCS SP5 laser-scanning confocal
559 microscope in resonant scanner mode. A region of interest (ROI) was selected
560 comprising an area between the epidermal flanks and the internalizing serosa,
561 corresponding to the extraembryonic amnion. The ROI was scanned for at least 30
562 seconds using a 405-nm UV laser and imaging was resumed after irradiation. Fixed,
563 immunostained embryos were imaged as follows: images were acquired using an
564 inverted Leica TCS SP5 laser-scanning confocal microscope. All post-acquisition
565 image processing and analysis was done using ImageJ software (NIH). For Voronoi
566 analysis, the center of mass of cell nuclei was detected manually with Fiji and used as
567 seed for Voronoi tessellation with Matlab.
568

Acknowledgments

We would like to thank Eva Jiménez-Guri, Karl Wotton, and Arturo D'Angelo for reagents and invaluable technical advice during the development of the project. We thank Steffen Lemke for providing training and technical advice as well as Jordi Casanova and Petra Stockinger for discussions and critical reading of the manuscript. All confocal imaging was done at the CRG Advanced Light Microscopy Unit. J.J.F-Z was supported by a CRG International Interdisciplinary Postdoctoral Programme (INTERPOD) fellowship, co-funded by Marie Curie Actions. We acknowledge support from the Spanish Ministry of Economy and Competitiveness (MINECO), 'Centro de Excelencia Severo Ochoa 2013-2017', SEV-2012-0208 and Plan Nacional BFU2015-68754-P.

Author contributions

J.J.F-Z. performed the experiments. J.J.F-Z. and J.S. performed the analysis. J.J.F-Z., J.S. and J.J. designed the research and wrote the manuscript.

Competing interests

The authors declare no competing financial or non-financial interests.

References

Bullock, S.L., Stauber, M., Prell, A., Hughes, J.R., Ish-Horowicz, D., Schmidt-Ott, U., 2004. Differential cytoplasmic mRNA localisation adjusts pair-rule transcription factor activity to cytoarchitecture in dipteran evolution. Development (Cambridge, England) 131, 4251-4261.

Campos-Ortega, J.A., Hartenstein, V., 1997. The embryonic development of Drosophila melanogaster. 2nd ed.

Carroll, S.B., Grenier, J.K., Weatherbee, S.D., 2009. From DNA to Diversity: Molecular Genetics and the Evolution of Animal Design. Wiley.

Chapman, R.F., 1998. The insects: structure and function, 4th ed. Cambridge University Press, Cambridge, UK ; New York, NY.

Crombach, A., Cicin-Sain, D., Wotton, K.R., Jaeger, J., 2012. Medium-throughput processing of whole mount in situ hybridisation experiments into gene expression domains. PLoS One 7, e46658.

Czerniak, N.D., Dierkes, K., D'Angelo, A., Colombelli, J., Solon, J., 2016. Patterned Contractile Forces Promote Epidermal Spreading and Regulate Segment Positioning during Drosophila Head Involution. Curr Biol 26, 1895-1901.

Davidson, E.H., Erwin, D.H., 2006. Gene regulatory networks and the evolution of animal body plans. Science 311, 796-800.

Ducuing, A., Keeley, C., Mollereau, B., Vincent, S., 2015. A DPP-mediated feed-forward loop canalizes morphogenesis during Drosophila dorsal closure. J Cell Biol 208, 239-248.

Eltsov, M., Dube, N., Yu, Z., Pasakarnis, L., Haselmann-Weiss, U., Brunner, D., Frangakis, A.S., 2015. Quantitative analysis of cytoskeletal reorganization during epithelial tissue sealing by large-volume electron tomography. Nat Cell Biol 17, 605-614.

Fernandez, B.G., Arias, A.M., Jacinto, A., 2007. Dpp signalling orchestrates dorsal closure by regulating cell shape changes both in the amnioserosa and in the epidermis. Mechanisms of development 124, 884-897.

Glise, B., Noselli, S., 1997. Coupling of Jun amino-terminal kinase and Decapentaplegic signaling pathways in Drosophila morphogenesis. Genes Dev 11, 1738-1747.

Hashimoto, H., Robin, F.B., Sherrard, K.M., Munro, E.M., 2015. Sequential contraction and exchange of apical junctions drives zippering and neural tube closure in a simple chordate. Dev Cell 32, 241-255.

Hilbrant, M., Horn, T., Koelzer, S., Panfilio, K.A., 2016. The beetle amnion and serosa functionally interact as apposed epithelia. Elife 5.

Horn, T., Hilbrant, M., Panfilio, K.A., 2015. Evolution of epithelial morphogenesis: phenotypic integration across multiple levels of biological organization. Front Genet 6, 303.

Hutson, M.S., Tokutake, Y., Chang, M.S., Bloor, J.W., Venakides, S., Kiehart, D.P., Edwards, G.S., 2003. Forces for morphogenesis investigated with laser microsurgery and quantitative modeling. Science 300, 145-149.

Jacinto, A., Martinez-Arias, A., Martin, P., 2001. Mechanisms of epithelial fusion and repair. Nat Cell Biol 3, E117-123.

649 Jacinto, A., Wood, W., Balayo, T., Turmaine, M., Martinez-Arias, A., Martin, P.,
650 2000. Dynamic actin-based epithelial adhesion and cell matching during Drosophila
651 dorsal closure. Curr Biol 10, 1420-1426.
652
653 Jacinto, A., Woolner, S., Martin, P., 2002. Dynamic analysis of dorsal closure in
654 Drosophila: from genetics to cell biology. Dev Cell 3, 9-19.
655
656 Jankovics, F., Brunner, D., 2006. Transiently reorganized microtubules are essential
657 for zippering during dorsal closure in Drosophila melanogaster. Dev Cell 11, 375-385.
658
659 Jimenez-Guri, E., Huerta-Cepas, J., Cozzuto, L., Wotton, K.R., Kang, H.,
660 Himmelbauer, H., Roma, G., Gabaldon, T., Jaeger, J., 2013. Comparative
661 transcriptomics of early dipteran development. BMC Genomics 14, 123.
662
663 Kaltschmidt, J.A., Lawrence, N., Morel, V., Balayo, T., Fernandez, B.G., Pelissier,
664 A., Jacinto, A., Martinez Arias, A., 2002. Planar polarity and actin dynamics in the
665 epidermis of Drosophila. Nat Cell Biol 4, 937-944.
666
667 Kato, K., Dong, B., Wada, H., Tanaka-Matakatsu, M., Yagi, Y., Hayashi, S., 2016.
668 Microtubule-dependent balanced cell contraction and luminal-matrix modification
669 accelerate epithelial tube fusion. Nat Commun 7, 11141.
670
671 Kiehart, D.P., Galbraith, C.G., Edwards, K.A., Rickoll, W.L., Montague, R.A., 2000.
672 Multiple forces contribute to cell sheet morphogenesis for dorsal closure in
673 Drosophila. J Cell Biol 149, 471-490.
674
675 Knust, E., 1997. Drosophila morphogenesis: movements behind the edge. Curr Biol 7,
676 R558-561.
677
678 Lecuit, T., Lenne, P.F., Munro, E., 2011. Force generation, transmission, and
679 integration during cell and tissue morphogenesis. Annu Rev Cell Dev Biol 27, 157-
680 184.
681
682 Mammoto, T., Ingber, D.E., 2010. Mechanical control of tissue and organ
683 development. Development (Cambridge, England) 137, 1407-1420.
684
685 Millard, T.H., Martin, P., 2008. Dynamic analysis of filopodial interactions during the
686 zippering phase of Drosophila dorsal closure. Development (Cambridge, England)
687 135, 621-626.
688
689 Monier, B., Pelissier-Monier, A., Brand, A.H., Sanson, B., 2010. An actomyosin-
690 based barrier inhibits cell mixing at compartmental boundaries in Drosophila
691 embryos. Nat Cell Biol 12, 60-65; sup pp 61-69.
692
693 Panfilio, K.A., 2008. Extraembryonic development in insects and the acrobatics of
694 blastokinesis. Dev Biol 313, 471-491.
695
696 Panfilio, K.A., Oberhofer, G., Roth, S., 2013. High plasticity in epithelial
697 morphogenesis during insect dorsal closure. Biol Open 2, 1108-1118.
698

699 Peter, I., Davidson, E.H., 2015. Genomic Control Process: Development and
700 Evolution. Elsevier Science.
701
702 Rafiqi, A.M., Lemke, S., Ferguson, S., Stauber, M., Schmidt-Ott, U., 2008.
703 Evolutionary origin of the amnioserosa in cyclorrhaphan flies correlates with spatial
704 and temporal expression changes of zen. Proc Natl Acad Sci U S A 105, 234-239.
705
706 Rafiqi, A.M., Lemke, S., Schmidt-Ott, U., 2010. Postgastrular zen expression is
707 required to develop distinct amniotic and serosal epithelia in the scuttle fly Megaselia.
708 Dev Biol 341, 282-290.
709
710 Rafiqi, A.M., Lemke, S., Schmidt-Ott, U., 2011a. Megaselia abdita: culturing and egg
711 collection. Cold Spring Harb Protoc 2011, pdb prot5600.
712
713 Rafiqi, A.M., Lemke, S., Schmidt-Ott, U., 2011b. Megaselia abdita: cuticle
714 preparation from injected embryos. Cold Spring Harb Protoc 2011, pdb prot5603.
715
716 Rafiqi, A.M., Lemke, S., Schmidt-Ott, U., 2011c. Megaselia abdita: fixing and
717 devitellinizing embryos. Cold Spring Harb Protoc 2011, pdb prot5602.
718
719 Rafiqi, A.M., Lemke, S., Schmidt-Ott, U., 2011d. Megaselia abdita: preparing
720 embryos for injection. Cold Spring Harb Protoc 2011, pdb prot5601.
721
722 Rafiqi, A.M., Park, C.H., Kwan, C.W., Lemke, S., Schmidt-Ott, U., 2012. BMP-
723 dependent serosa and amnion specification in the scuttle fly Megaselia abdita.
724 Development (Cambridge, England) 139, 3373-3382.
725
726 Rauzi, M., Krzic, U., Saunders, T.E., Krajnc, M., Ziherl, P., Hufnagel, L., Leptin, M.,
727 2015. Embryo-scale tissue mechanics during Drosophila gastrulation movements. Nat
728 Commun 6, 8677.
729
730 Rothwell, W.F., Sullivan, W., 2000. Fluorescent analysis of Drosophila embryos.
731 Drosophila protocols, 141-157.
732
733 Saias, L., Swoger, J., D'Angelo, A., Hayes, P., Colombelli, J., Sharpe, J., Salbreux,
734 G., Solon, J., 2015. Decrease in Cell Volume Generates Contractile Forces Driving
735 Dorsal Closure. Dev Cell 33, 611-621.
736
737 Schmidt-Ott, U., Kwan, C.W., 2016. Morphogenetic functions of extraembryonic
738 membranes in insects. Current Opinion in Insect Science 13, 86-92.
739
740 Schmidt-Ott, U., Sander, K., Technau, G.M., 1994. Expression of engrailed in
741 embryos of a beetle and five dipteran species with special reference to the terminal
742 regions. Roux's archives of developmental biology 203, 298-303.
743
744 Sluss, H.K., Han, Z., Barrett, T., Goberdhan, D.C., Wilson, C., Davis, R.J., Ip, Y.T.,
745 1996. A JNK signal transduction pathway that mediates morphogenesis and an
746 immune response in Drosophila. Genes Dev 10, 2745-2758.
747

Sommi, P., Cheerambathur, D., Brust-Mascher, I., Mogilner, A., 2011. Actomyosin-dependent cortical dynamics contributes to the prophase force-balance in the early Drosophila embryo. PLoS One 6, e18366.

Stauber, M., Taubert, H., Schmidt-Ott, U., 2000. Function of bicoid and hunchback homologs in the basal cyclorrhaphan fly Megaselia (Phoridae). Proc Natl Acad Sci U S A 97, 10844-10849.

VanHook, A., Letsou, A., 2008. Head involution in Drosophila: genetic and morphogenetic connections to dorsal closure. Dev Dyn 237, 28-38.

Wells, A.R., Zou, R.S., Tulu, U.S., Sokolow, A.C., Crawford, J.M., Edwards, G.S., Kiehart, D.P., 2014. Complete canthi removal reveals that forces from the amnioserosa alone are sufficient to drive dorsal closure in Drosophila. Mol Biol Cell 25, 3552-3568.

Wilkins, A.S., 2002. The Evolution of Developmental Pathways. Sinauer Associates.

Wotton, K.R., Jimenez-Guri, E., Crombach, A., Janssens, H., Alcaine-Colet, A., Lemke, S., Schmidt-Ott, U., Jaeger, J., 2015. Quantitative system drift compensates for altered maternal inputs to the gap gene network of the scuttle fly Megaselia abdita. Elife 4.

Wotton, K.R., Jimenez-Guri, E., Garcia Matheu, B., Jaeger, J., 2014. A staging scheme for the development of the scuttle fly Megaselia abdita. PLoS One 9, e84421.

Figure Legends

Figure 1. The extraembryonic serosa ruptures and accumulates dorsally previous to epidermal seaming in *Megaselia abdita*. (A) Nuclear staining of *M. abdita* embryos prior to dorsal closure reveals three types of tissues: the extraembryonic serosa (magenta), the extraembryonic amnion (blue), and the embryonic epidermis (gray). **(A')** An orthogonal re-sliced stack along the dashed yellow line in A shows the position of the embryonic (gray), amniotic (blue), and serosal (magenta) tissues in transverse view. **(B)** Schematics depicting the organization of the serosa cells (magenta), amnion cells (blue), and embryonic epidermis (green) in lateral and **(B')** transverse view. The black dashed line represents the vitelline envelope **(C)** *M. abdita* embryo undergoing rupture and retraction of serosal tissue along the ventral side. Staining against β-tubulin in green, and DAPI nuclear counterstain in magenta. **(D)** Serosal cells (magenta arrowheads) accumulate on the dorsal side of the embryo after rupture. The serosa remains apposed to the amnion (blue arrowheads), which is in turn apposed to the embryonic epidermis (white arrowheads). Phalloidin stain in green and DAPI nuclear counterstain in magenta. **(E)** Images from a time-lapse sequence of serosa retraction in a *M. abdita*

798 embryo injected with the fluorescent lipophilic dye FM 4-64 (from video 1). Yellow
799 dashed line shows the contour of the serosa covering the embryo during retraction. **(F)**
800 Relative changes in area of the serosa during retraction (red, *n*=15 embryos), and
801 relative changes in height (*h*) of the dorsal opening (blue, *n*=15 embryos) during
802 dorsal closure in *M. abdita*. Vertical bars represent standard deviation (SD). Time
803 range of dorsal ridge fusion is represented by pink area (*n*=15 embryos) as a landmark
804 for the initiation of dorsal closure. The origin of the time axis (*T=0* min) is set at the
805 point of serosa rupture. **(G)** Schematics depict transverse views of embryos during
806 serosa rupture, retraction, and dorsal accumulation. Serosal cells rupture along the
807 ventral end of the embryo (red arrowhead). **(G')** The remaining lateral serosa cells
808 retract towards the dorsal side (black arrows). **(G'')** Serosa cells continue retracting
809 until they completely accumulate onto the dorsal opening (black arrows). Color
810 scheme as in B. In all embryos and schematics, dorsal is to the top. Embryos in A, C,
811 D and E show lateral views where anterior is to the left.
812
813 **Figure 1— supplement 1. Identification of extraembryonic tissues in *Megaselia***
814 ***abdita*. (A)** Confocal projection of nuclear staining in an intact *M. abdita* embryo
815 stained with DAPI. **(A')** Confocal projection and image processing of nuclear staining
816 from A to separate the extraembryonic serosa (magenta) and extraembryonic amnion
817 (blue) from the embryonic epidermis. **(B)** Confocal projection to observe the
818 discontinuous DAPI staining in serosa cells (magenta dashed line) and continuous
819 DAPI staining in amnion cells (blue dashed line). **(B')** Plotted intensity profiles of the
820 serosa and amnion showing the discontinuous and continuous DAPI stainings,
821 respectively. **(B'')** Nuclear size (measured as area in μm^2) of serosa cells (average
822 size 125± 21 μm^2, SD, *n*=150 cells), amnion cells (average size 77 ± 16 μm^2, SD,
823 *n*=150 cells) and epidermal cells (average size 14 ± 3 μm^2, SD, *n*=150 cells). **(C-C'')**
824 Dorsal view of three sequential *z*-stack confocal images (0, -4 and -6 µm) in a live *M.*
825 *abdita* embryo injected with DAPI and showing the localization of amnion cells on
826 yolk granules and adjacent to the epidermis (blue arrowheads). In all embryos,
827 anterior is to the left.
828
829 **Figure 1— supplement 2. Description of the three-tissue system anatomy in**
830 ***Megaselia abdita* prior to dorsal closure. (A)** Nuclear staining (DAPI) of serosa
831 cells (magenta) attached to the vitelline membrane after devitellinization. **(B)**
832 Phalloidin staining (green) of a devitellinized embryo (dorsal view) showing a gap on
833 the dorsal side of the embryo left by serosa removal with intact embryonic epidermis
834 and adjacent amnion cells (blue arrowheads). **(C)** Lateral view of a devitellinized
835 embryo where a couple of serosa cells (white arrowhead) and amnion cells (blue
836 arrowhead) remained intact after removal of the vitelline membrane. This embryo
837 corresponds to an early stage of dorsal closure prior to serosa rupture (*T≈0* min) as
838 indicated by large intact serosa cells, the fused dorsal ridge at the anterior end of the
839 dorsal opening, a straightened epidermal leading edge and the large height (*h*) of the
840 dorsal opening. **(C')** Higher magnification of the embryo in D at the site where
841 extraembryonic serosa (white arrowhead) and amnion (blue arrowhead) remained
842 intact upon devitellinization. **(C'')** Orthogonal stack re-slicing along the white dashed
843 line in D showing a cross-section of the three-tissue anatomy of *M. abdita* dorsal
844 closure where amnion cells (blue arrowheads) and serosa cells (white arrowheads) are
845 apposed (yellow arrowhead). In embryos from A to C' anterior is to the left. In
846 embryos from C to C'', dorsal is to the top.
847

Figure 1— supplement 3. Anatomical landmarks during dorsal closure progression and serosa internalization. (A-A'') Dorsal views from a time-lapse sequence of dorsal closure in a *M. abdita* embryo labeled with the fluorescent dye FM 4-64. Magenta bands depict the position and fusion of the dorsal ridge during the early and mid phase of dorsal closure. Yellow solid lines show the scalloped perimeter of the dorsal opening during early phase (A), the straightened perimeter during mid phase (A'), and the seamed epidermis during late phase (A'') of dorsal closure. Yellow dotted line shows the dorsal midline and the blue solid line depicts the measured height (*h*) of the dorsal opening during dorsal closure. **(a-a'')** Raw images from A-A'' without superimposed labels. In all embryos, anterior is to the left. **(B-B'')** Dorsal (top) and orthogonal (bottom) views from a time-lapse sequence of a FM 4-64-labeled *M. abdita* embryo during dorsal closure during mid (B) and late (B'-B'') phase of dorsal closure (from video 2). The magenta arrow in bottom panel indicates the extraembryonic serosa cells undergoing apicobasal elongation towards the yolk and undergoing internalization. Anterior is to the top in dorsal view and dorsal is to the top in orthogonal view. **(C-C')** Time-lapse images (from top panel of video 7) showing the apicobasal elongation of the serosa during its retraction and internalization. In (C), the yellow area indicates the yolk and the magenta dashed lines highlight serosal apico-basal junctions. (C') represents the same sequence without labels.

Figure 2. JNK (*bsk*) is required for *dpp* expression and the completion of dorsal closure without affecting serosa rupture or retraction in *Megaselia abdita*. (A) Wild-type expression of *Mab_dpp* (purple stain, black arrowheads) along the dorsal leading edge of the epidermis in a *M. abdita* embryo (lateral view) during dorsal closure. **(A')** Cuticle preparation of a wild-type late-stage pre-hatching *M. abdita* embryo (dorsal view). **(B)** RNAi knock-down of *Mab_bsk* abolishes *Mab_dpp* expression at the leading edge of the epidermis (magenta arrowheads) in a *M. abdita* embryo (lateral view). **(B')** Cuticle preparation of a *Mab_bsk* RNAi late-stage pre-hatching embryo, showing a dorsal-open phenotype (magenta arrowheads). **(C)** Images from a bright-field time-lapse sequence of serosa retraction in a *M. abdita* embryo treated with *Mab_bsk* RNAi (from video 3). Yellow dashed lines show the perimeter of the serosa covering the embryo during retraction. In all embryos and cuticles anterior is to the left and dorsal to the top.

Figure 2— supplement 1. *Mab_bsk* RNAi results in a lack of dorsal closure progression after serosa rupture. (A-A'') Detection of the serosa edge in the bright-field time-lapse sequence of *Mab_bsk* knock-down embryo from figure 2C was obtained by image subtraction **(a-a'')** to render the retracting serosa visible (magenta arrowheads). **(B)** *Mab_bsk* knock-down results in a sclerotized cuticle at the leading edge of the epidermis (yellow arrowheads) in late-stage pre-hatching embryos. This phenotype is due to the lack of dorsal closure progression. Note this embryo is the same as the embryo in the time-lapse sequence in figure 2C, C' and C'' and video 3, 24 hours after dsRNA injection.

Figure 3. An actomyosin-enriched epidermal cable is necessary for the completion of dorsal closure upon contraction, retraction, and internalization of the serosa in *Megaselia abdita*. (A) F-actin enrichment (as observed by inverted intensity of phalloidin staining) and **(B)** PhosphoMyosin enrichment (inverted intensity of immunostaining) in the epidermal leading edge (green arrowhead) and

internalizing serosa (red arrowhead), but not in the amnion (blue arrowhead) of a *M. abdita* embryo during dorsal closure. **(C–C'')** Time series of different phalloidin-stained *M. abdita* embryos that show merging of both amniotic and epidermal flanks brought together at the dorsal midline upon serosa internalization. Amniotic merging (blue arrowheads) is visible by a transient accumulation of F-actin (white arrowhead in C''). Epidermal merging is mediated by the actomyosin cable (yellow arrowheads). **(D)** Average area of the serosa during retraction in wild-type control (red, *n*=15 embryos), and contractility-impaired embryos injected with Y-27632 (purple, *n*=15 embryos). The latter show delayed and incomplete serosal retraction and ingression. Vertical bars represent standard deviations (SD). Embryos from A to D are in dorsal view where anterior is to the left. Embryo in D' is an optical transverse view where dorsal is to the top.

Figure 3— supplement 1. Actin accumulates apically in contracting serosa cells and filopodial protrusions are present in the epidermal actin cable of *Megaselia abdita*. **(A)** Lateral view of a *M. abdita* embryo showing F-actin accumulation at the epidermal leading edge and the internalizing serosa (red arrowheads), but not in the extraembryonic amnion (blue arrowheads). **(B)** Serosa cell surface area reduces over time during contraction from an average of 212 ± 52 μm^2 (SD; *n*= 20 cells) to 76 ± 18 μm^2 (SD; *n*= 20 cells) to 33 ± μm^2 (SD; *n*= 20 cells) at 20, 30 and 40 min after serosa rupture, respectively. **(C-C''')** Dorsal view of phalloidin-stained *M. abdita* embryos at different stages of serosa internalization with their corresponding orthogonal stack re-slicing **(c-c''').** F-actin accumulates preferentially at the apical part of contracting serosa cells (white arrowhead) during internalization. White dashed line in C-C''' depicts the site of optical re-slicing. In A and C, phalloidin staining in green and DAPI counterstain in magenta. In A anterior is to the left and dorsal to the top. In C anterior is to the top and in c dorsal is to the top. **(D)** and **(D')** Filopodia-like structures (yellow arrowheads) extend from the epidermal cable towards the dorsal midline as evidenced in dorsal view of a *M. abdita* embryo. Phalloidin staining in green. In D and D'' anterior is to the left.

Figure 3— supplement 2. The epidermal actomyosin cable is a contractile structure controlled by JNK (*Mab_bsk*) expression during dorsal closure.
(A) An actomyosin cable (white arrowhead) at the epidermal leading edge of a wild-type *M. abdita* embryo. **(B)** *Mab_bsk* RNAi results in the absence of an actomyosin cable (white arrowhead) in *M. abdita* embryos during dorsal closure. **(C)** Downregulation of the actomyosin cable (white arrowhead) after injection of the Rho kinase (ROCK) inhibitor Y-27632. From A to C, embryos are labeled with phalloidin staining in green and DAPI nuclear counterstain in magenta. Anterior is to the left and dorsal to the top. **(D-D'')** Kinetics of serosal retraction in embryo injected with the Rho-kinase inhibitor Y-27632. Drug treatment arrests the progression of the epidermal leading edge (magenta arrowheads) and abolishes the dorsal internalization of the serosa cells **(E-E'')** Dorsal and transversal views of the retraction of the serosa in Y-27632 treated embryos. The inward bending and apicobasal cell elongation of the serosa are prevented and disruption of the tissue occurs without apparent contraction**.** Embryos in D and E are taken from time-lapse sequences of FM 4-64-labeled embryos from videos 4 and 5, respectively. In D, anterior is to the left and dorsal to the top. In E, the top panel is a dorsal view with anterior to the top and the bottom panel is a transversal view with dorsal to the top.

Figure 4. Microtubule-dependent seaming of the extraembryonic amnion is required for subsequent epidermal seaming during dorsal closure in *Megaselia abdita*. **(A)** Confocal projections of microtubules in the extraembryonic amnion orienting towards the internalizing serosa during early amniotic seaming. **(B)** As amniotic seaming progresses, microtubules maintain alignment, and become localized apically, as revealed by a transverse view **(B')**, obtained by orthogonal stack re-slicing along the blue line in B. Staining against β-tubulin is shown in green, DAPI nuclear counterstain in magenta. **(C)** Time-lapse sequence of amniotic seaming (blue dashed line and blue shaded area) followed by epidermal seaming (green dashed line) along the dorsal midline in a *M. abdita* embryo injected with the fluorescent lipophilic dye FM 4-64 (from video 6). **(D)** Time-lapse sequence of dorsal closure in a colcemid treated embryo to induce microtubule depolymerization. After serosa retraction the process is arrested and closure fails. The embryo is labeled by FM 4-64 (from video 8). White arrowheads in D show the proper straightening of the epidermal leading edge in colcemid-injected embryos. Red arrowhead in D'' indicates impaired serosa internalization. **(E)** Relative changes in height (*h*) of dorsal opening during in wild-type control (blue, *n*=15 embryos) and embryos injected with colcemid (red, *n*=15 embryos) to depolymerize microtubules. Vertical bars show standard deviations (SD). These measurements reveal failed epidermal leading edge progression in colcemid-treated *M. abdita* embryos. **(F)** Schematics depicting the transverse view (top) and dorsal view (bottom) of embryos during serosa cell ingression, initiation of amnion cell elongation, and microtubule alignment (purple) towards the dorsal midline. Black arrows indicate the direction of amnion progression. **(F')** Amnion cells show alignment of apical microtubule bundles towards the dorsal midline, where the two amniotic flanks meet, and amniotic seaming occurs (dark blue line). This is followed by the progression of the epidermal leading edge (dark green arrows), which results in epidermal seaming and completion of dorsal closure (not shown). Serosa in magenta, amnion in blue and embryonic epidermis in green. All embryo images show dorsal views where anterior is to the left.

Figure 4— supplement 1. Microtubule alignment is present in both the epidermis and the amnion and correlates with enlarged amniotic cells in *Megaselia abdita*. **(A)** Microtubule bundles orient towards the dorsal midline (white dashed line) in both the epidermis (white arrowhead) and the amnion (blue arrowhead) of *M. abdita* embryos during dorsal closure. Note that microtubules in the internalizing serosa lack a clear orientation (red arrowhead). **(B)** At the epidermal leading edge of *M. abdita* embryos, microtubule bundles orient dorsoventrally (white arrowheads) and show apical localization as revealed by a transverse view **(B')** obtained by orthogonal stack re-slicing along the yellow line in B. **(C-C''')** A timed series of fixed embryos shows that microtubule alignment (blue arrowheads) and amnion cell elongation are maintained during serosa internalization (C) and the merging of amnion cells from opposite flanks (C'). Amnion microtubule alignment is lost after the opposite amnion flanks meet at the dorsal midline (C''). In A-C, β-tubulin staining in green and DAPI nuclear counterstain in magenta. **(D)** Estimated apical cell surface area by Voronoi tessellation around the nuclei of extraembryonic cells stained with DAPI. Amnion cells (blue arrowheads) present an elongated apical cell surface area compared to serosa cells (red arrowheads). In all embryos, anterior is to the left.

Figure 4— supplement 2. Colcemid treatment prevents microtubule polymerization without affecting serosa retraction or epidermal actomyosin

cable in *Megaselia abdita*. (A) Average area of serosa during retraction in wild-type control embryos (blue, *n*=10 embryos) and colcemid-injected (red, *n*=10 embryos). Kinetics of serosa retraction did not show an apparent difference in treated embryos compared to wild-type control. Vertical bars represent standard deviations (SD). **(B)** Epidermal actomyosin cable (white arrowheads) and contracting serosa (magenta arrowheads) in colcemid-injected embryos do show similar F-actin enrichment than wild type during the initial stages of internalization. The embryo is in dorsal view. Anterior is to the left. **(B')** Higher magnification of B showing F-actin accumulation in the epidermal cable (white arrowheads) and the contracting serosa (magenta arrowhead). β-tubulin staining in green, phalloidin counterstain in magenta and DAPI counterstain in blue. **(C-C')** Orthogonal views from a time-laspe sequence of colcemid-injected *M. abdita* embryos labeled with FM 4-64 (from bottom panel of video 7). Colcemid-treated embryos undergo serosa internalization and apicobasal cell elongation towards the yolk similarly than wild type. The yellow area in C highlights the yolk region and the dashed magenta lines highlight serosa cell apicobasal junctions. C' shows the sequence in C without annotations. Dorsal is to the top. **(D)** Colcemid injection during dorsal closure induces microtubules depolymerization in *M. abdita* embryos as observed in both the leading edge of the epidermis (white arrowhead) and the extraembryonic amnion (blue arrowhead) compared to a wild-type non injected embryo **(D')**. β-tubulin staining in green. Anterior is to the left.

Figure 4— supplement 3. UV-deactivation of colcemid in the amnion region allows dorsal closure progression in treated *Megaselia abdita* embryos. (A) (Left panel) Dorsal view of a *M. abdita* wild-type control embryo injected with FM 4-64 during serosa accumulation at the dorsal opening. Yellow dashed line represents the edge of the epidermal flanks. (Right panel) Dorsal closure is completed 60 minutes after the initiation of serosa internalization. **(A')** (Left panel) Dorsal view of a colcemid injected embryos labeled with FM 4-64 during serosa accumulation at the dorsal opening. (Right panel) 60 minutes after, dorsal closure does not progress and the epidermal flanks remain open. **(A'')** (Left panel) Dorsal view of a colcemid injected embryos labeled with FM 4-64 in which UV light is irradiated in a region between the epidermal flanks and the internalizing serosa (magenta shaded area, corresponding to the amnion) of colcemid-injected embryos. (Right panel) Dorsal closure progressed further in UV-irradiated embryos, although the epidermis did not close completely after 60 minutes of serosa internalization. Yellow dashed lines indicate the epidermal leading edge **(B)** Relative changes in height (*h*) of dorsal opening in wild-type control embryos (white bar; 4 ± 1%, *n*= 10 embryos), colcemid-injected embryos (blue bar; 90 ± 21%, *n*= 10 embryos) and colcemid-treated/UV-irradiated embryos (magenta bar; 19 ± 7%, *n*= 10 embryos). Error bars are standard deviations (SD). These measurements indicate a rescue of dorsal closure progression after UV-deactivation of colcemid in *M. abdita* injected embryos.

Figure 4— supplement 4. Landmarks of amniotic seaming during dorsal closure progression in *Megaselia abdita*. (A-A'') Lateral view from two time-lapse sequences of dorsal closure progression in *M. abdita* embryos labeled with FM 4-64 (from video 9). Top panels show a wild-type embryo undergoing serosa accumulation (A), amnion cell elongation (A') and epidermal edge progression towards the dorsal midline (A''). Bottom panels show a *M. abdita* embryo treated with colcemid undergoing serosa accumulation, amnion cell elongation and further retraction of the epidermal leading edge from the dorsal midline. In all embryos, dorsal is at the top.

(B-B'') Dorsal view from a time-lapse sequence of amniotic seaming (blue dashed line and blue shaded area) followed by epidermal seaming (green dashed line) along the dorsal midline in a *M. abdita* embryo injected with FM 4-64 (from video 6). **(b-b'')** Raw images from B-B'' without superimposed labels. In all embryos, anterior is to the left.

Video 1. Dorsal closure in *Megaselia abdita* involves the rupture and retraction of the serosa and advancement of the epidermal flanks to the dorsal midline. Time-lapse sequence of dorsal closure in two *M. abdita* embryos injected with the fluorescent label FM 4-64. Top: serosa rupture and retraction in lateral view. Rupture initiates at a ventral-posterior location and spreads anteriorly along the ventral side of the embryo. The ruptured serosa accumulates on the dorsal side, where epidermal seaming occurs at the end of dorsal closure. Bottom: dorsal view of the initiation of dorsal closure, marked by the fusion of the dorsal ridge and straightening of the epidermal leading edge (see figure 1— supplement 3A). Epidermal flanks are brought together to the dorsal midline where epidermal seaming occurs. In both embryos, anterior is to the left.

Video 2. The extraembryonic serosa of *Megaselia abdita* embryos internalizes into the yolk prior to epidermal seaming. Time-lapse sequence of a dorsal (top) and orthogonal view (bottom) of an FM 4-64-labeled embryo. After serosa rupture and accumulation at the dorsal opening, the extraembryonic tissue internalizes into the yolk, as observed by an inward bending of the tissue and apicobasal cell elongation. Upon internalization of the serosa, the epidermal flanks advance and fuse at the dorsal midline. In the dorsal view, anterior is to the top. In the orthogonal view, dorsal is to the top.

Video 3. Knock-down of *Mab_bsk* by RNAi does not prevent serosa rupture and retraction despite preventing epidermal flanks from closing in *Megaselia abdita* embryos. Bright-field time-lapse sequence of serosa retraction in a *M. abdita* embryo injected with *Mab_bsk* dsRNA at early stages of development. Knock-down of *Mab_bsk* does not impair serosa rupture and retraction despite preventing embryos from closing the dorsal hole. Embryo in lateral view. Anterior is to the left, dorsal to the top.

Video 4. Injection of the Rho kinase inhibitor Y-27632 prevents dorsal closure and slows down serosa retraction in *Megaselia abdita*. Time-lapse sequence of dorsal closure in a FM 4-64 labeled *M. abdita* embryo injected with the Rho kinase (ROCK) inhibitor Y-27632, which downregulates actomyosin-based contractility. Note the slow rupture and retraction of the serosa, and the failure of the epidermal flanks to advance and close. Embryo in side view where anterior is to the left, dorsal to the top. Note that the static stains observed are stains on the vitelline envelope arising from embryo treatment prior to imaging.

Video 5. Injection of the Rho kinase inhibitor Y-27632 prevents internalization of the serosa in *Megaselia abdita* embryos. Time-lapse sequence of a dorsal (top) and orthogonal view (bottom) of serosa rupture in an FM 4-64 labeled *M. abdita* embryo. Injection of the Rho kinase (ROCK) inhibitor Y-27632 (to downregulate actomyosin-based contractility) prevents internalization of the serosa. The inward bending and apicobasal cell elongation of the extraembryonic tissue into the yolk is

not observed in orthogonal view. In the dorsal view, anterior is to the top. In the orthogonal view, dorsal is to the top. Note that the static stains observed are stains on the vitelline envelope arising from embryo treatment prior to imaging.

Video 6. Amniotic seaming followed by epidermal seaming during the late stage of dorsal closure in *Megaselia abdita*. Time-lapse sequence of the final stage of dorsal closure in a *M. abdita* embryo fluorescently labeled with FM 4-64. The amnion flanks are brought together and seamed at the dorsal midline upon serosa ingression. This process is followed by seaming of the epidermal flanks at the dorsal midline. Both seaming processes initiate at the posterior end of the embryo. Embryo in dorsal view. Anterior is to the left. Note that the static stains observed are stains on the vitelline envelope arising from embryo treatment prior to imaging.

Video 7. The initial stages of serosa internalization in colcemid-injected embryos of *Megaselia abdita* occur as in wild-type embryos. Time-lapse sequence in orthogonal view of dorsal closure during serosa internalization in FM 4-64-labeled *M. abdita* embryos. The inward bending of the extraembryonic tissue and apicobasal cell elongation into the yolk is observed in wild-type control (top) and colcemid-injected embryos (bottom). Injection of colcemid induces microtubule polymerization and impairs the late stages of dorsal closure (see video 8). Dorsal is to the top.

Video 8. Colcemid injection prevents dorsal closure in *Megaselia abdita*. Time-lapse sequence of impaired dorsal closure in an FM 4-64-labeled *M. abdita* embryo after injection of colcemid to induce microtubule depolymerization. The initial stages of dorsal closure (straightening of the epidermal leading edge and serosa rupture and retraction) are not affected. The process of dorsal closure is aborted during the late stages (amniotic seaming and epidermal seaming). Embryo in dorsal view. Anterior is to the left.

Video 9. Colcemid injection impairs amniotic flank seaming during dosal closure in *Megaselia abdita.* Time-lapse sequence in lateral view of the latest stages of dorsal closure in FM 4-64-labeled *M. abdita* embryos. Amnion cell elongation can be observed in a wild-type embryo (top) resulting in the seaming of the amniotic flanks followed by seaming of the epidermal flanks. In colcemid-injected embryos (bottom), amnion cells initially elongate but fail to maintain elongation and retract from the amniotic merging at the dorsal midline. Note that the static stains observed are stains on the vitelline envelope arising from embryo treatment prior to imaging.

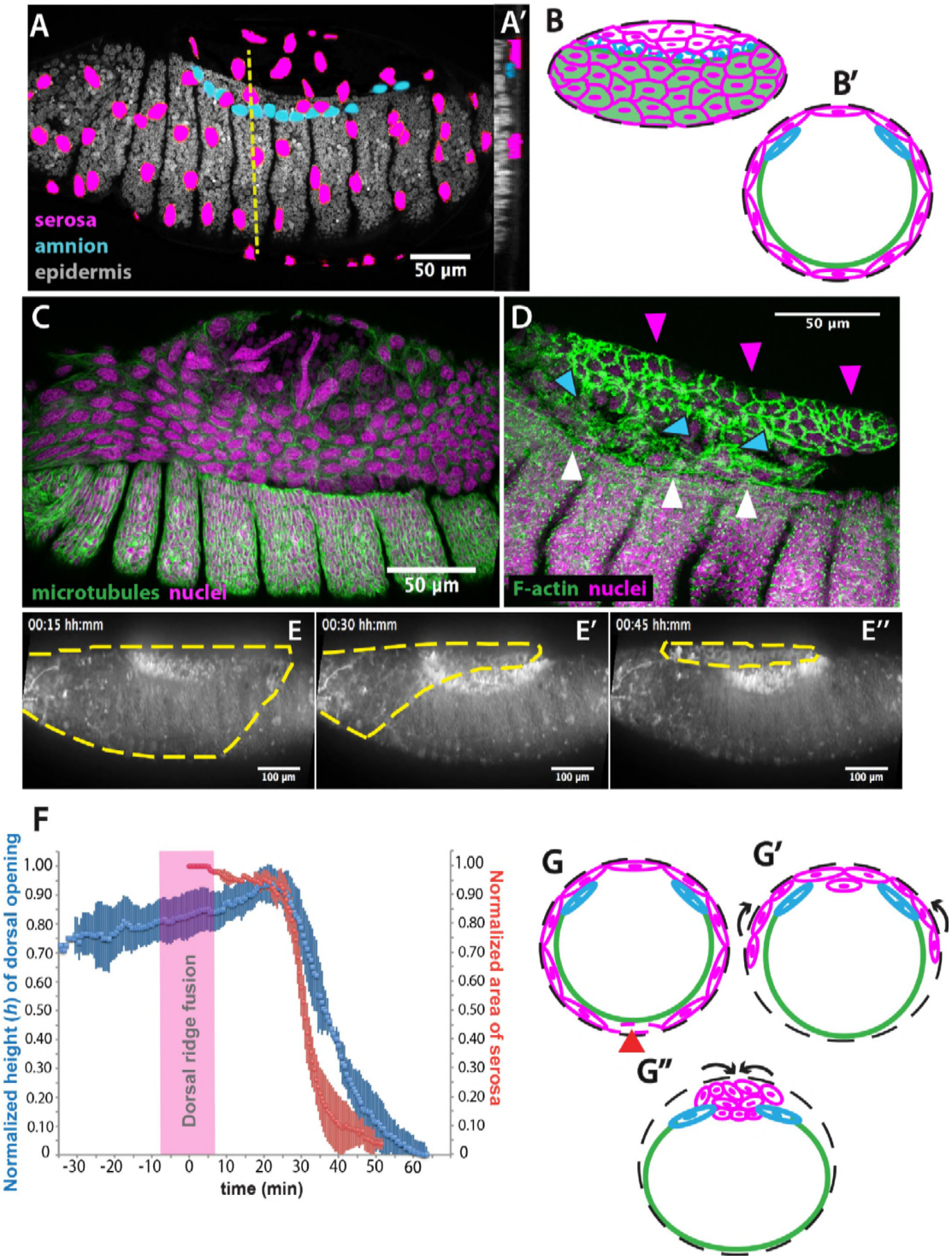

Figure 1.

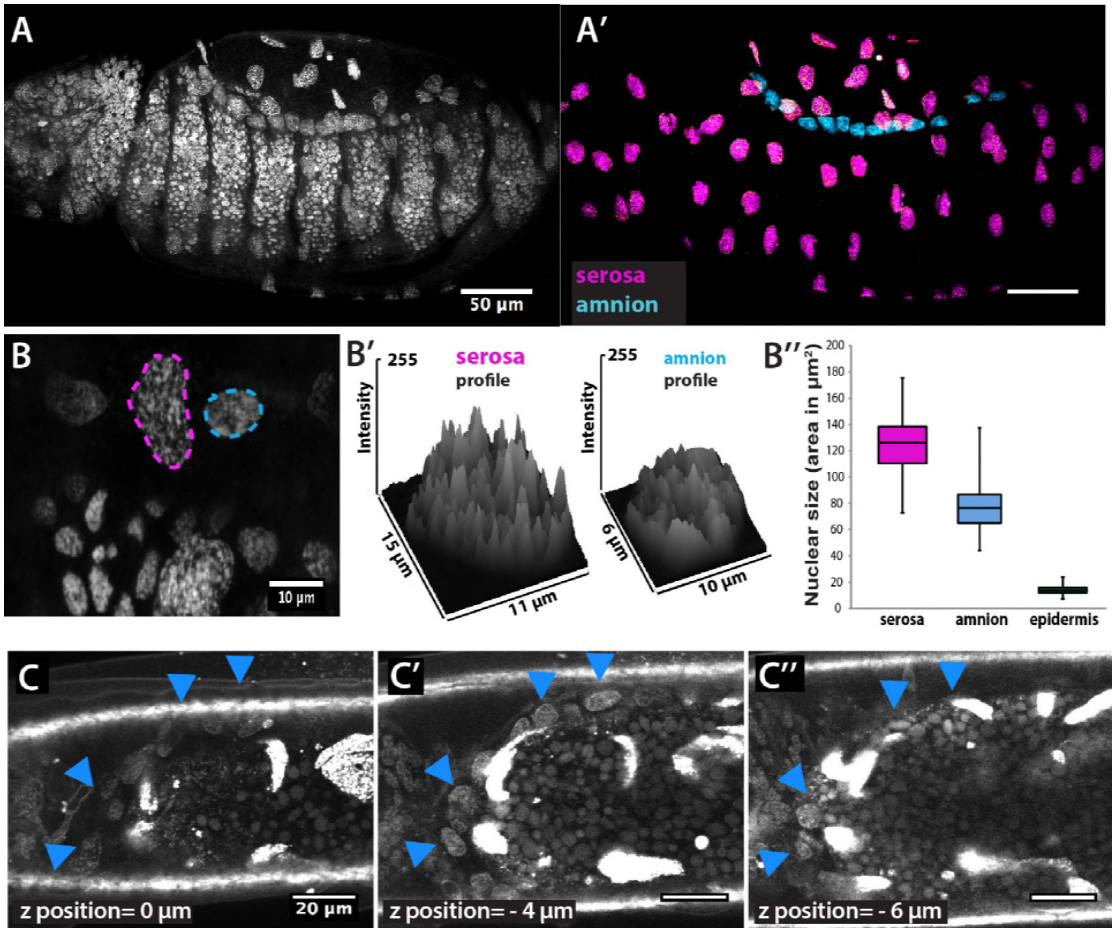

Figure 1— supplement 1.

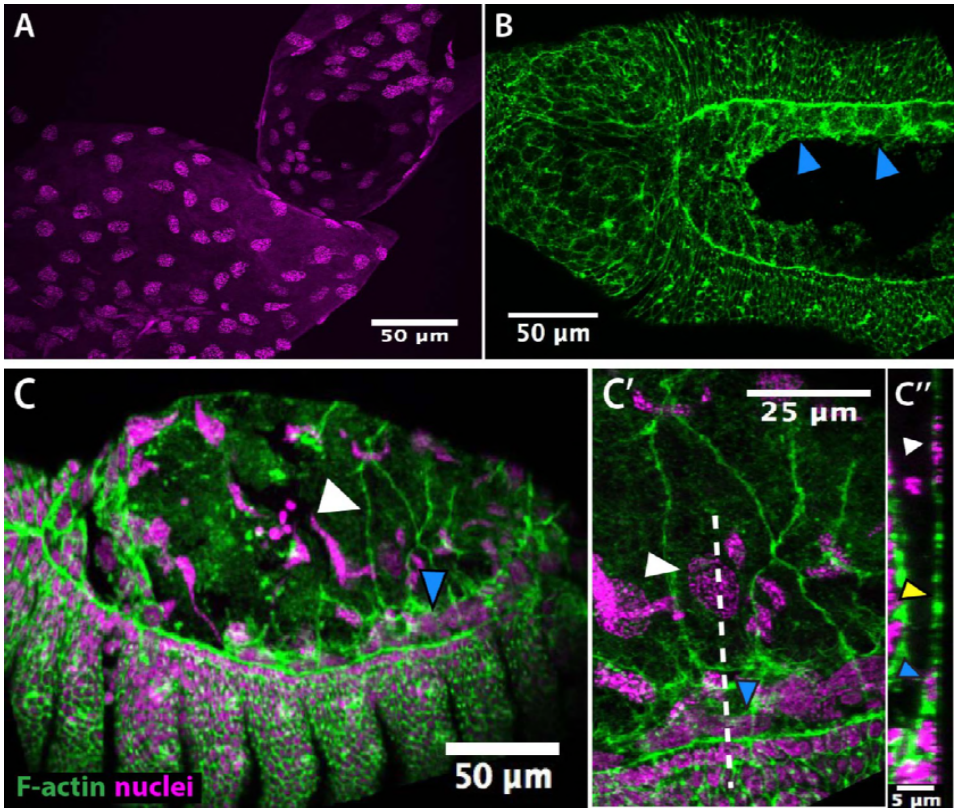

Figure 1— supplement 2.

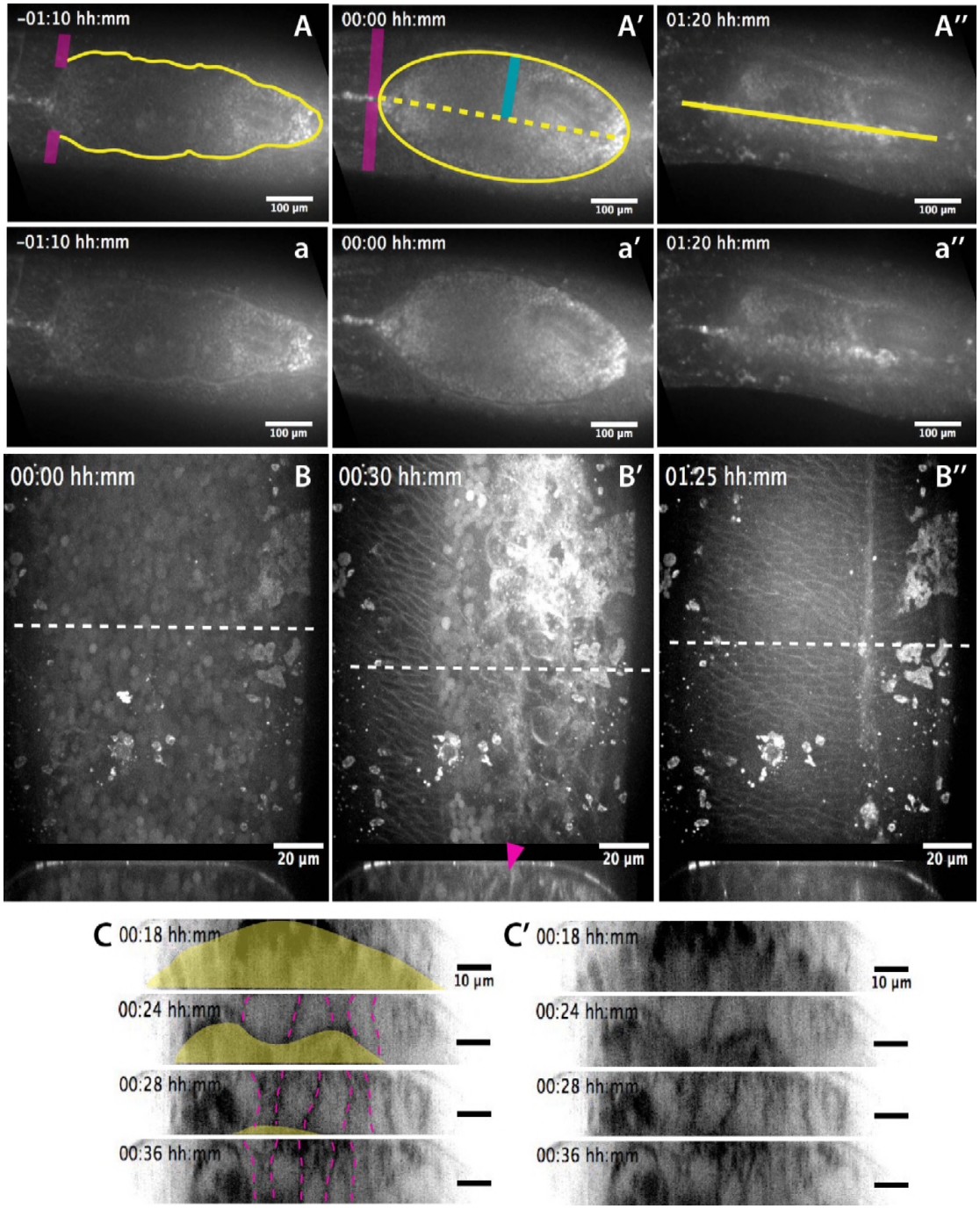

Figure 1— supplement 3.

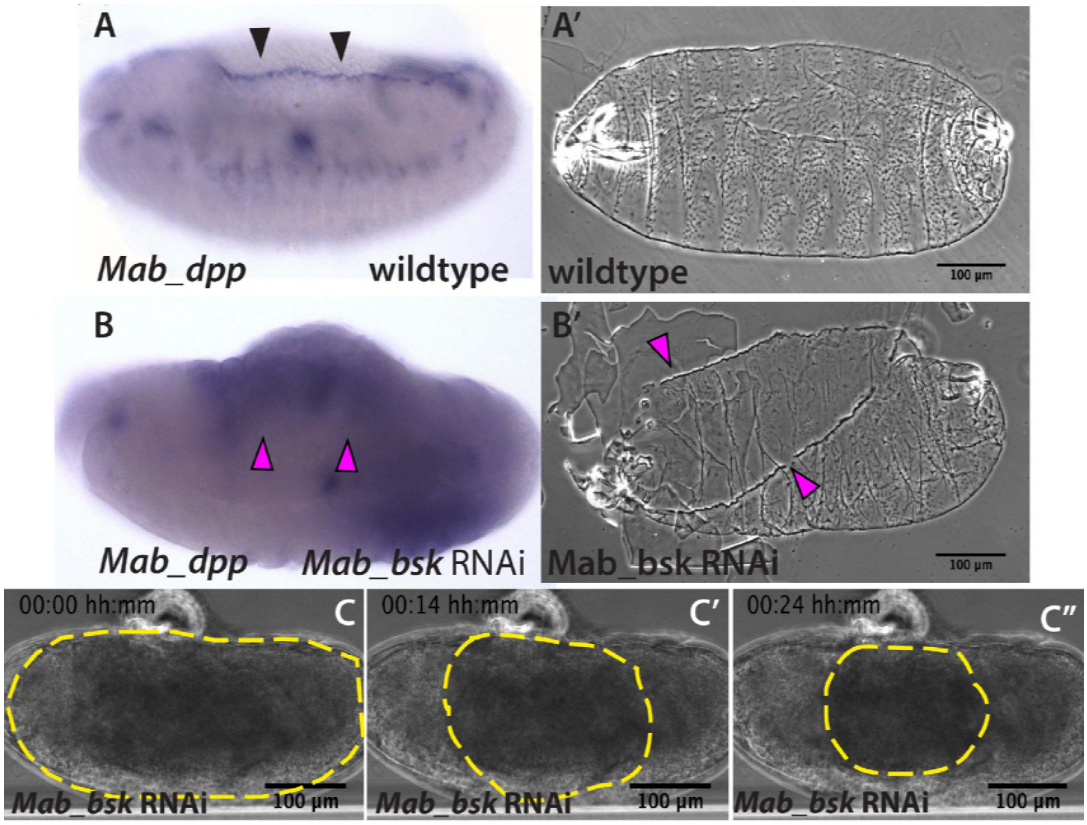

Figure 2.

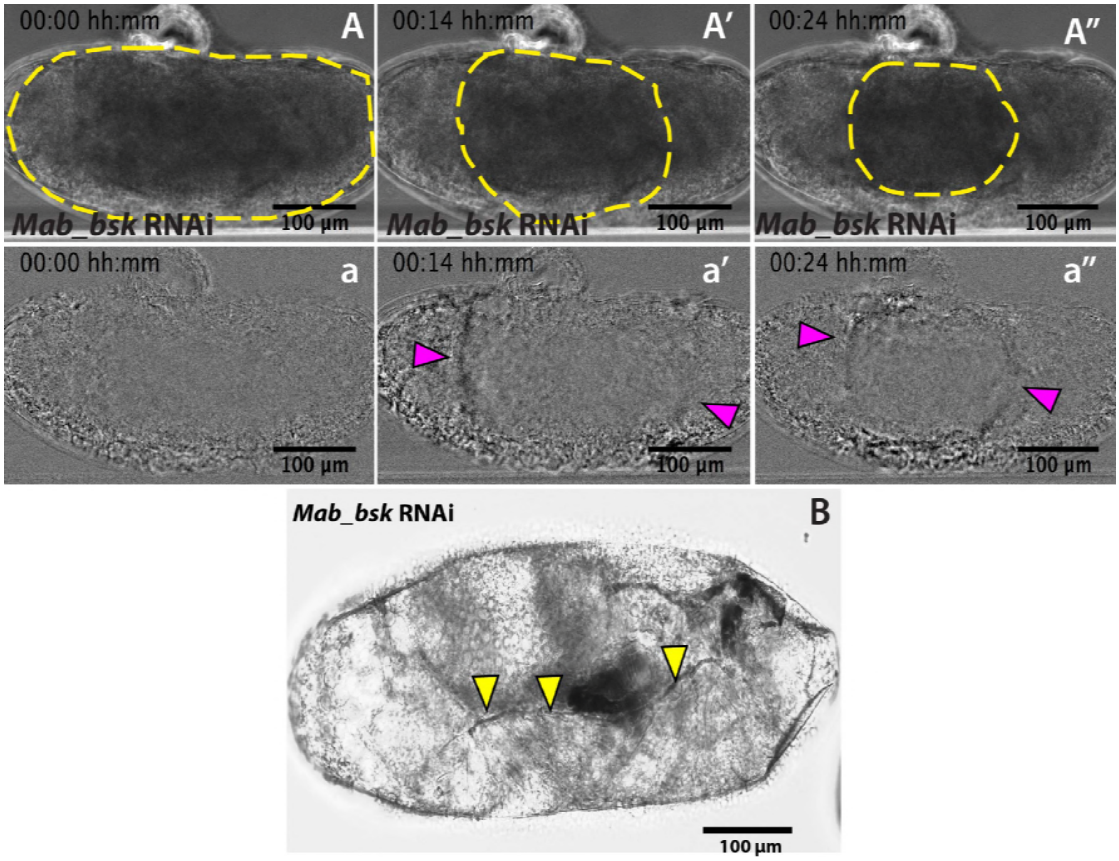

Figure 2— supplement 1.

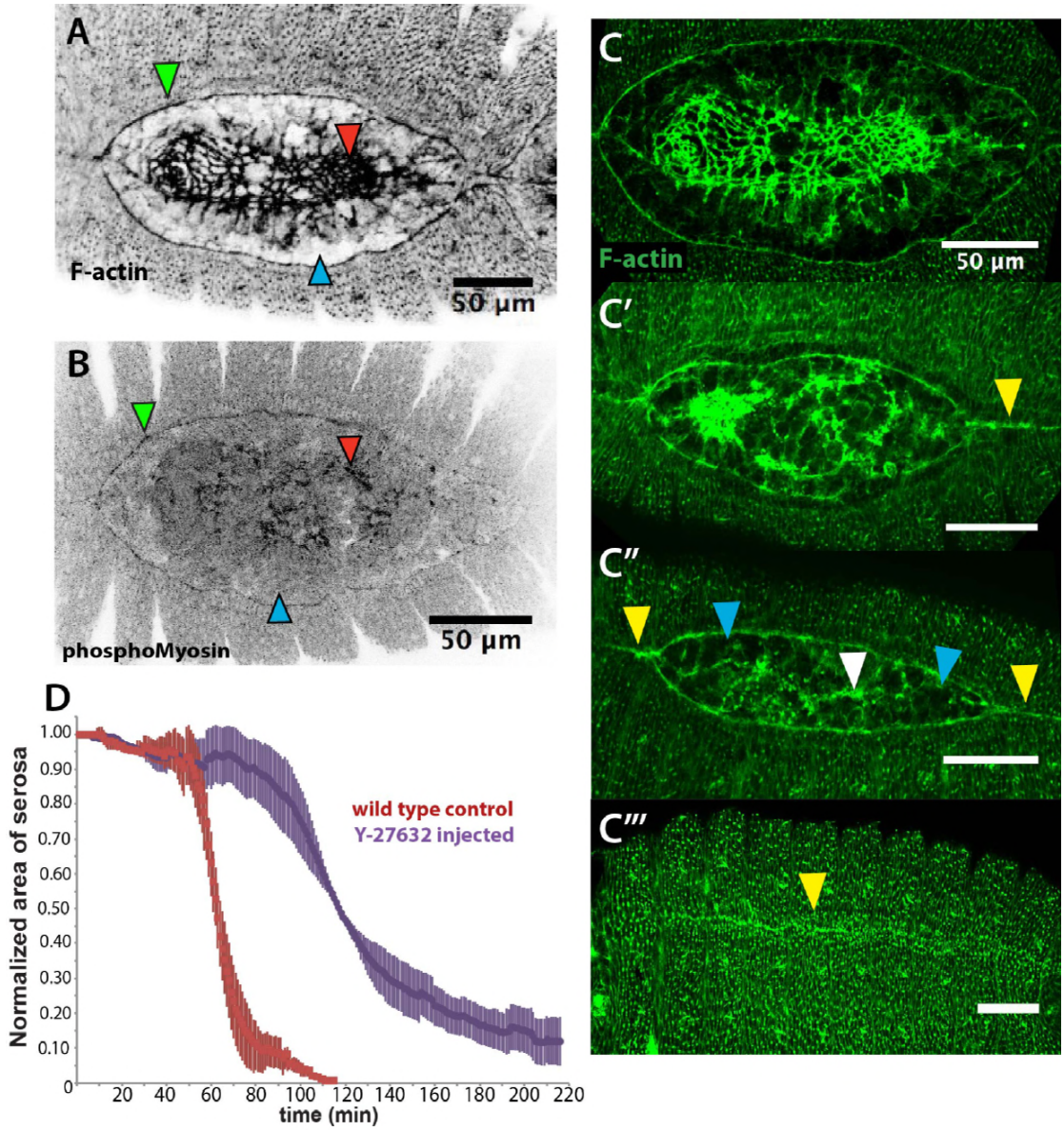

Figure 3.

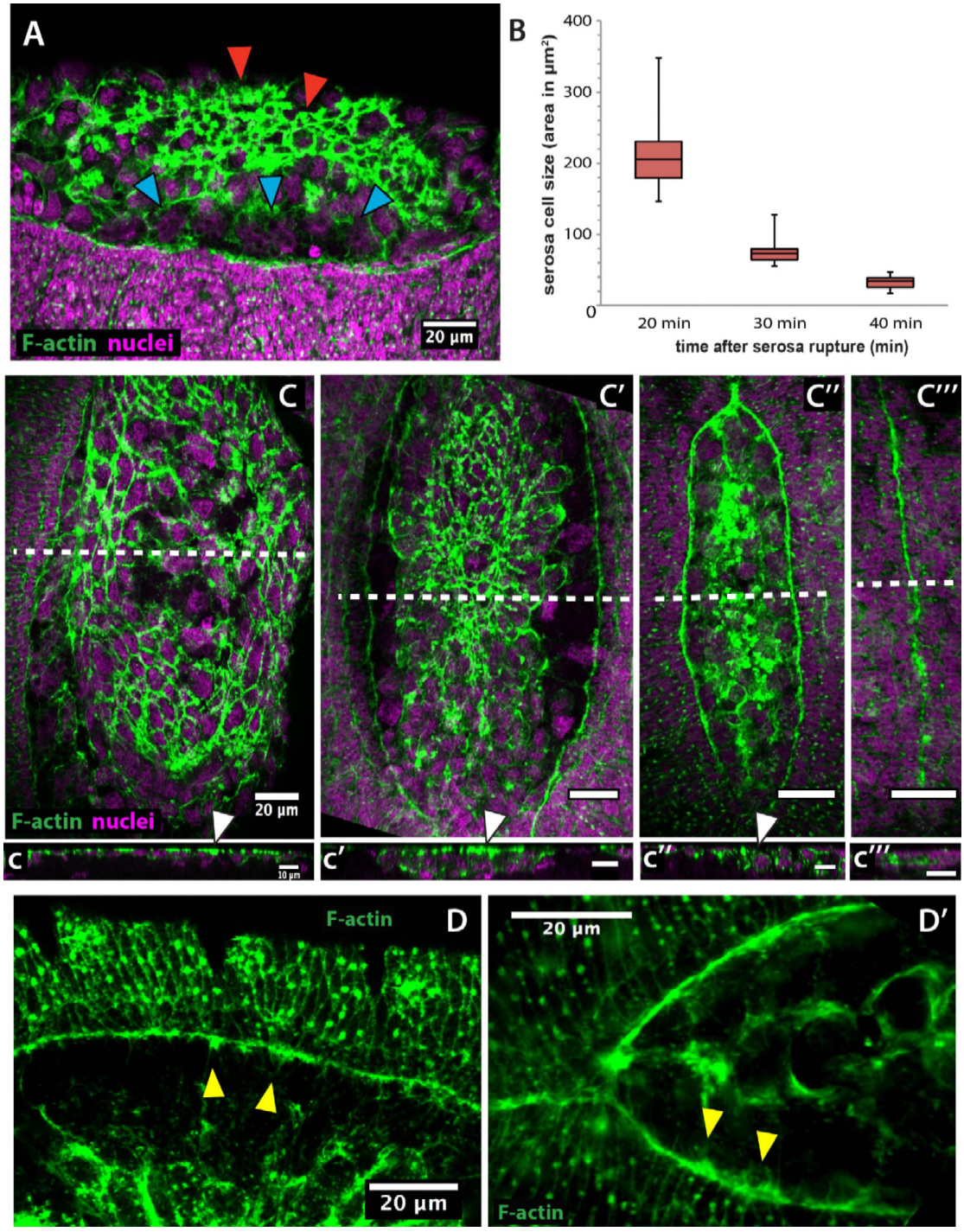

Figure 3— supplement 1.

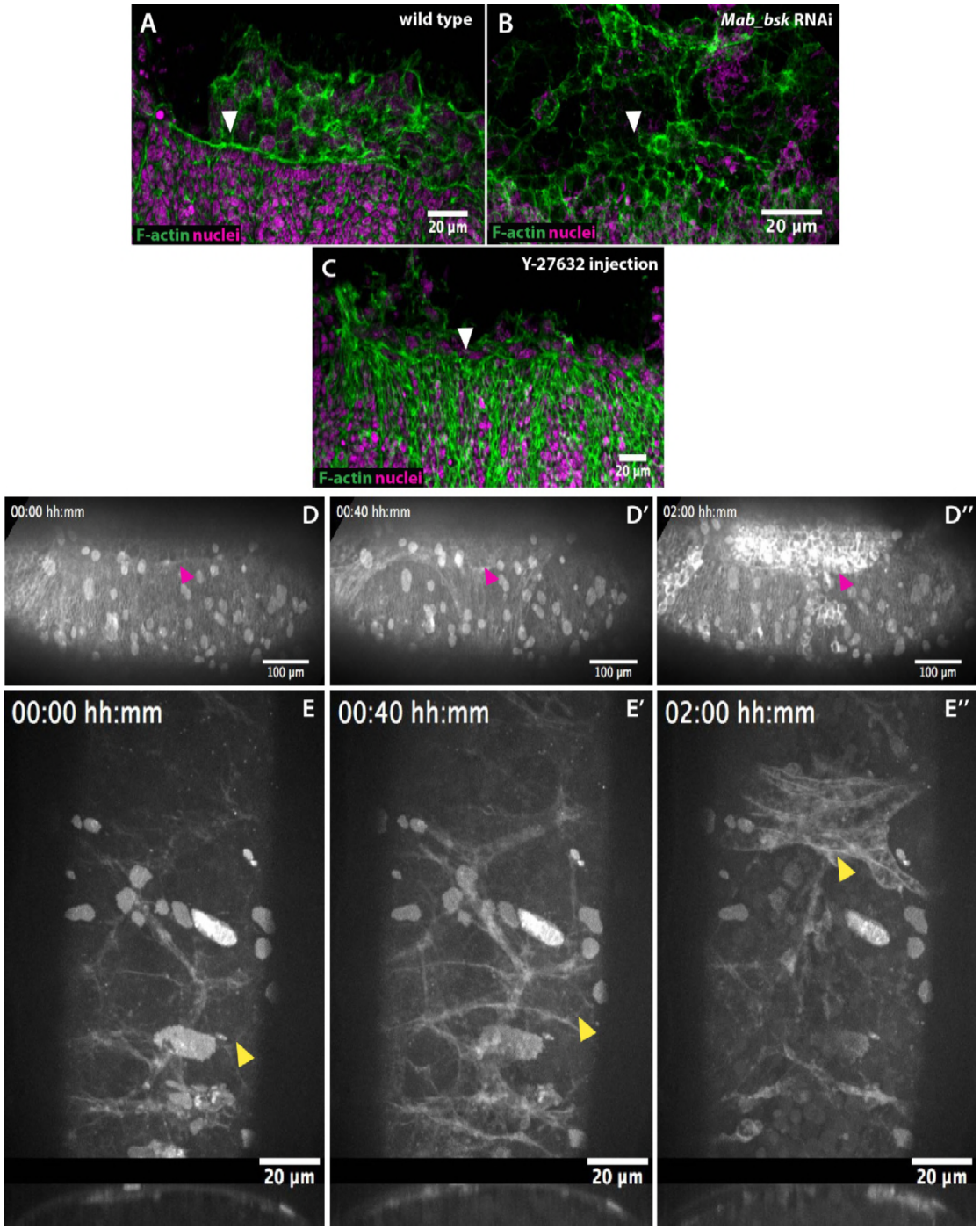

Figure 3— supplement 2.

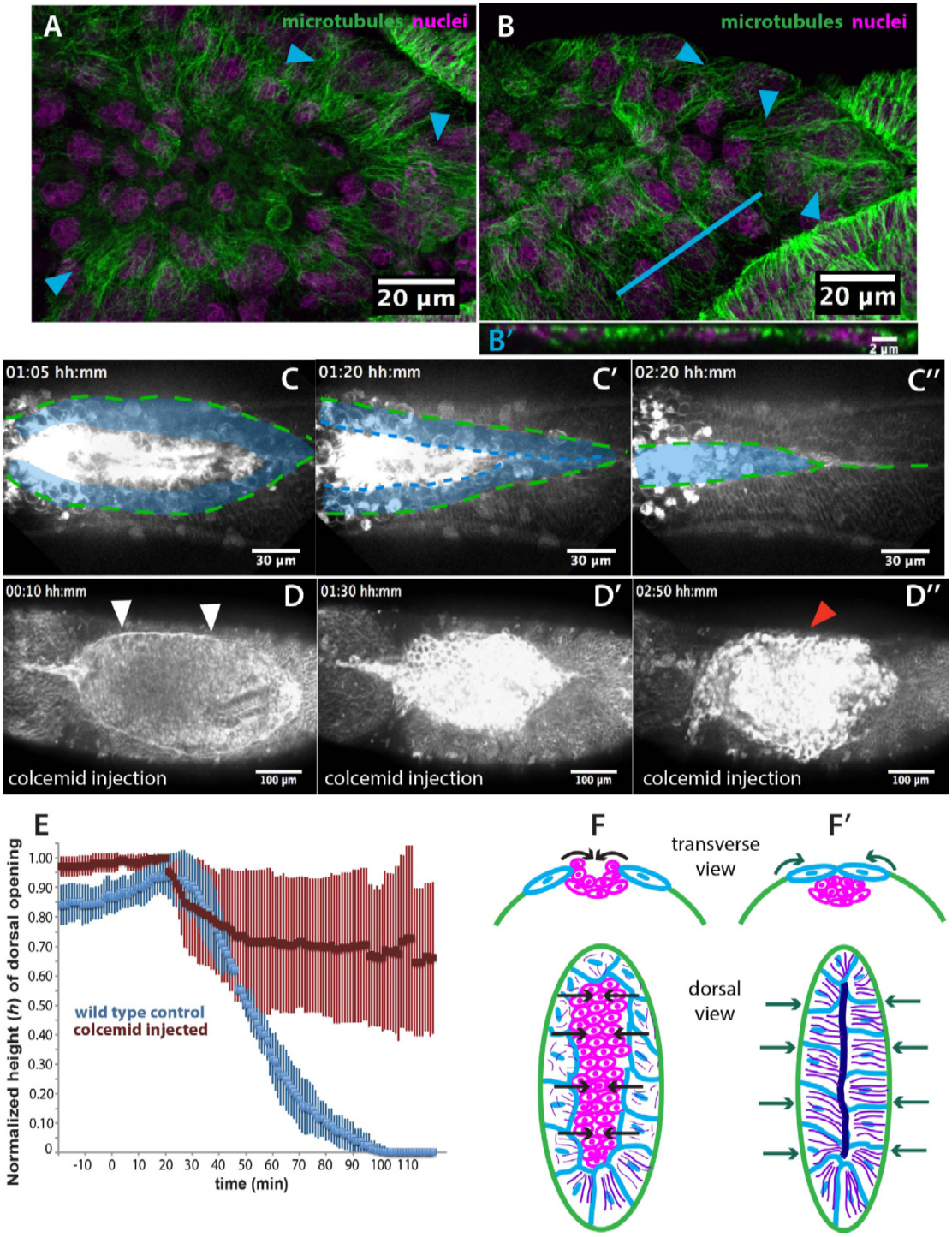

Figure 4.

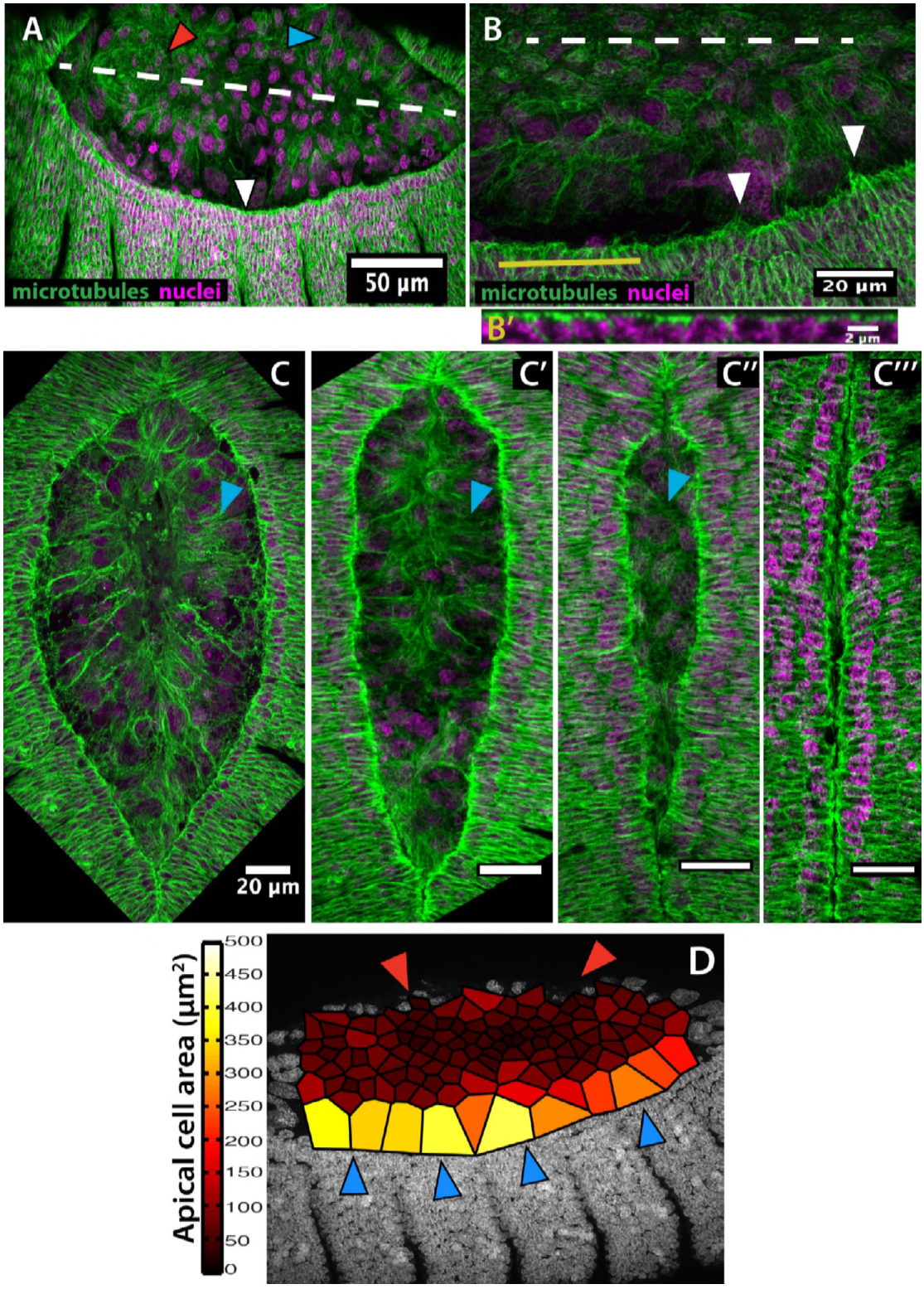

Figure 4— supplement 1.

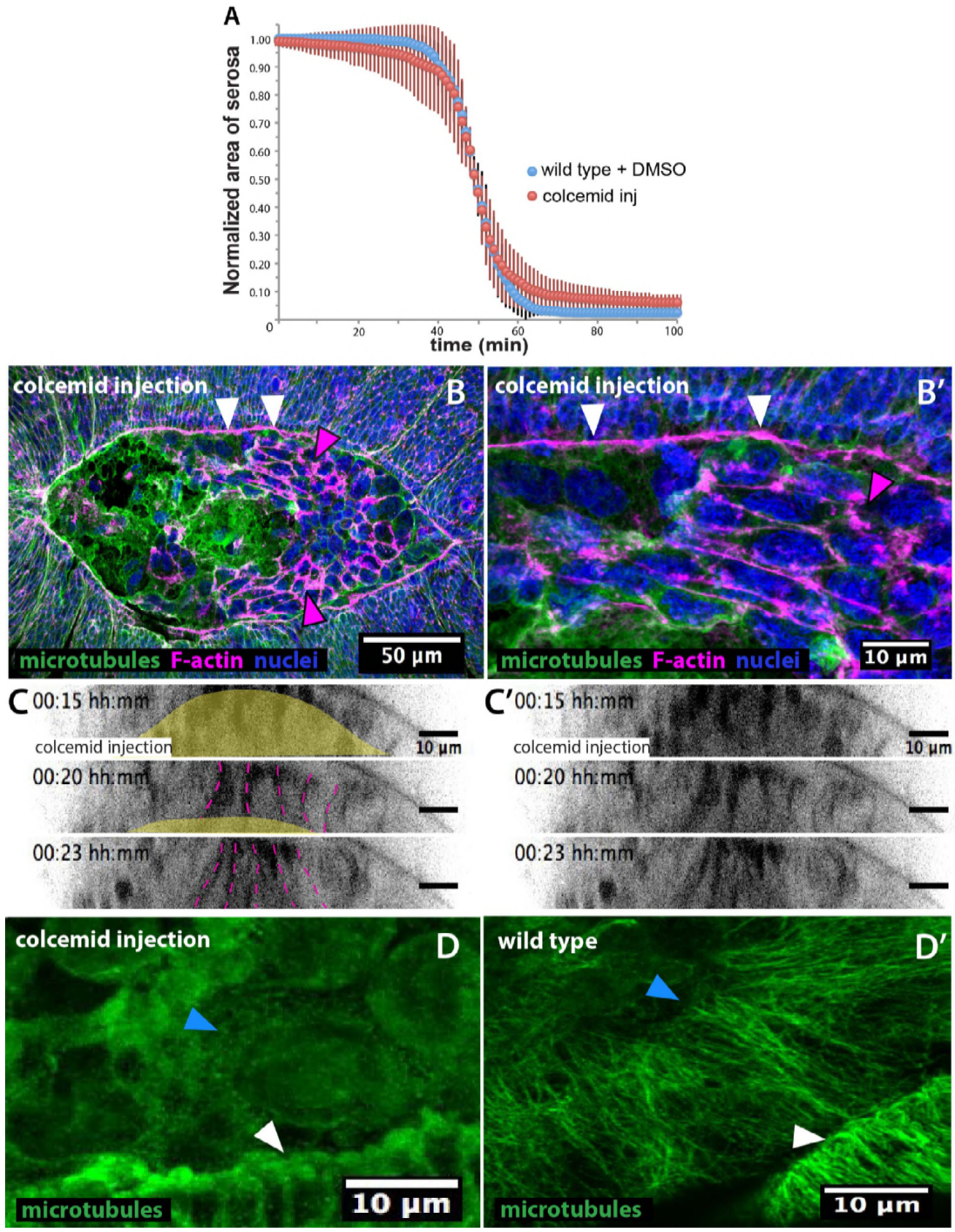

Figure 4— supplement 2.

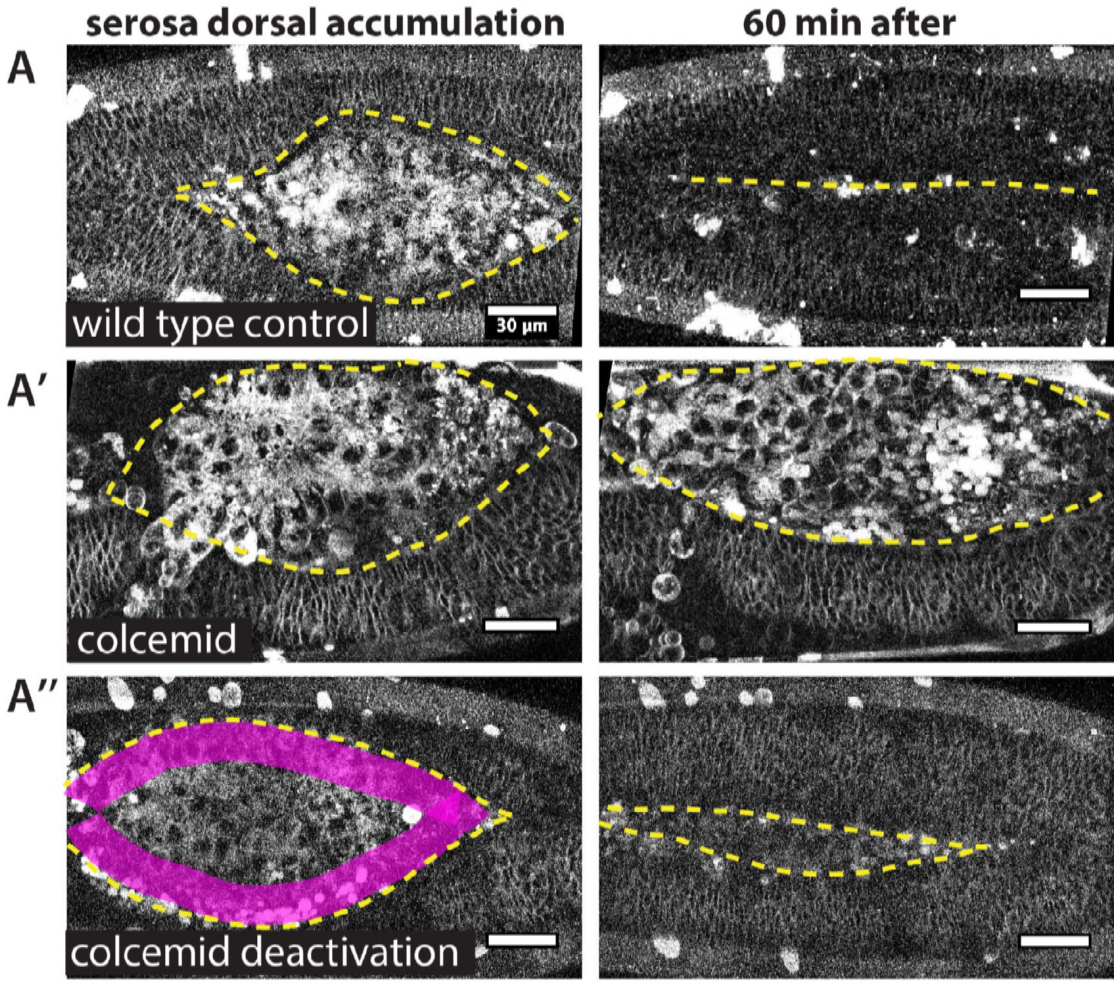

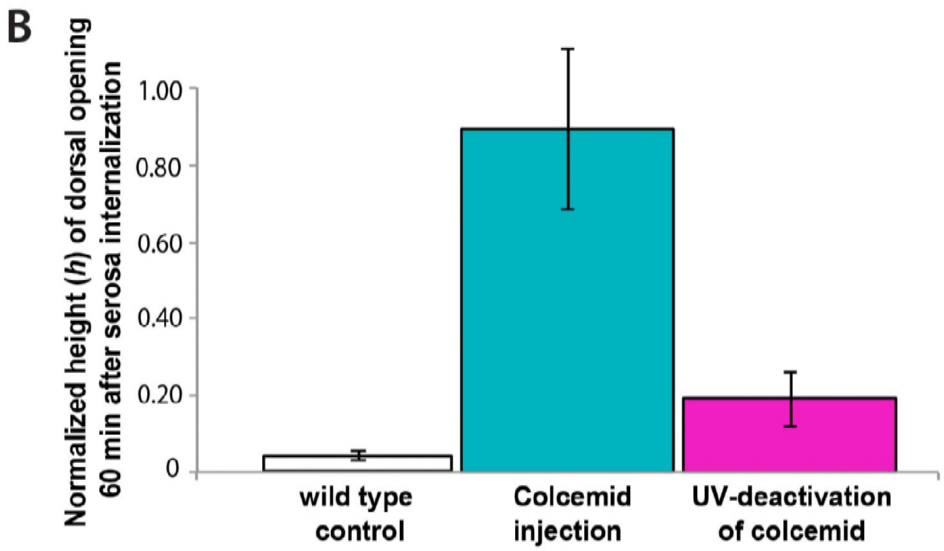

Figure 4— supplement 3.

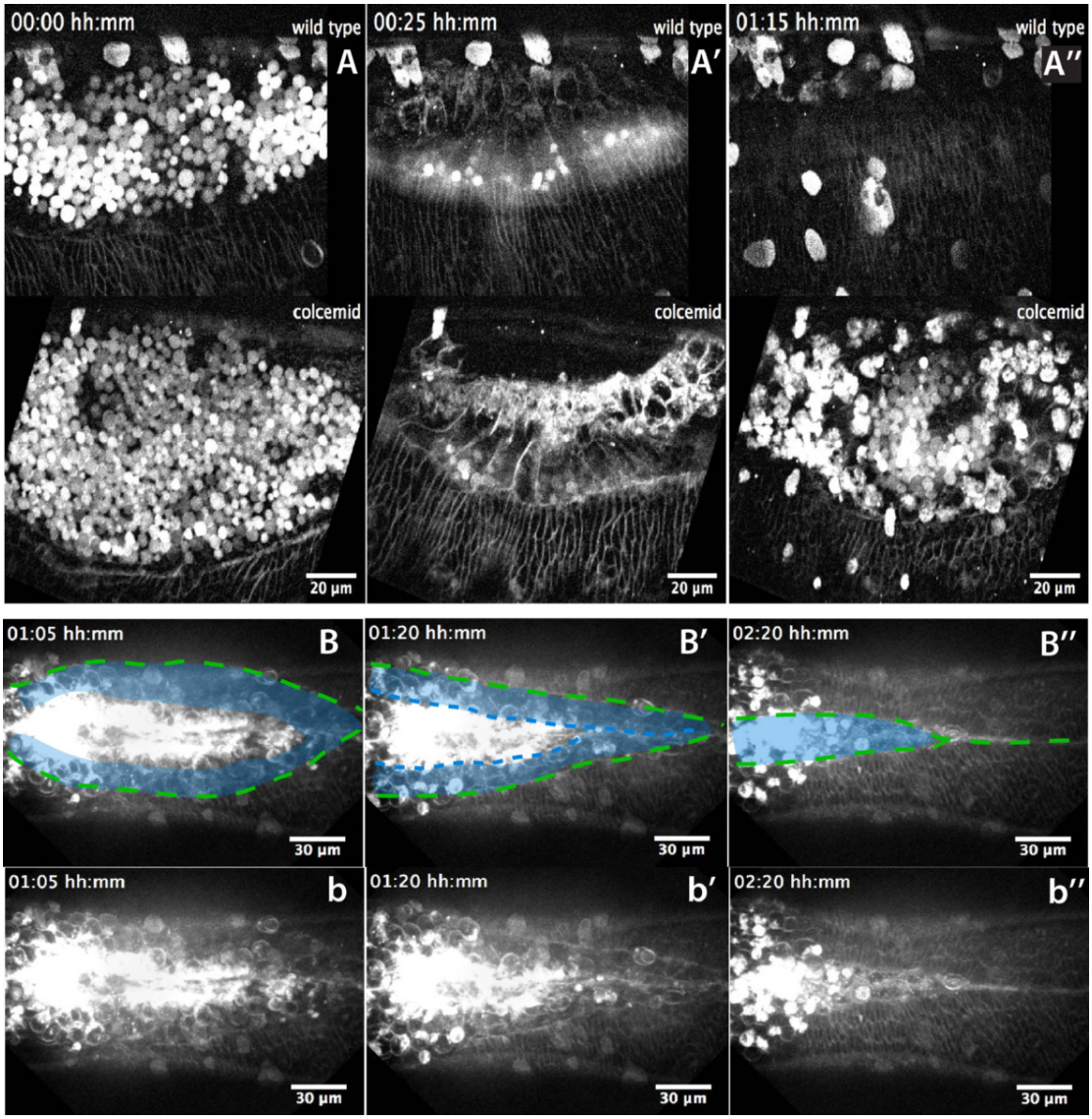

Figure 4— supplement 4.